

Fast Converging Path Integrals for Time-Dependent Potentials

Antun Balaž,^{1,*} Ivana Vidanović,¹ Aleksandar Bogojević,¹ and Axel Pelster^{2,3}

¹*Scientific Computing Laboratory, Institute of Physics Belgrade, Pregrevica 118, 11080 Belgrade, Serbia[†]*

²*Fachbereich Physik, Universität Duisburg-Essen, Lotharstraße 1, 47048 Duisburg, Germany*

³*Universität Potsdam, Campus Golm, Karl-Liebknecht-Straße 24/25, 14476 Potsdam-Golm, Germany*

We calculate the short-time expansion of the propagator for a general quantum system with many degrees of freedom in a time-dependent potential to orders that have not been accessible before. To this end the propagator is expressed in terms of a discretized effective potential, for which we derive and analytically solve a set of efficient recursion relations. Such a discretized effective potential can be used to substantially speed up numerical Monte-Carlo simulations for path integrals, or to set up various analytic approximation techniques to study dynamic properties of quantum systems in time-dependent potentials. The analytically derived results are numerically verified by treating several simple models in both imaginary and real time.

PACS numbers: 05.30.-d, 02.60.-x, 05.70.Fh, 03.65.Db

Keywords: Time-dependent potential, Evolution operator, Effective action, Many-body system

I. INTRODUCTION

Studying quantum systems in time-dependent potentials represents a fundamental problem which emerges in many areas of physics. Even if the Hamiltonian of the system itself does not explicitly depend on time, such situations naturally occur in the presence of time-dependent external fields. Another important example are fast-rotating systems, where the rotation introduces an explicit time dependence of the respective variables in the co-rotating frame. This includes modern experiments with rotating ultracold atoms and Bose-Einstein condensates [1–5], studies of vortices [6, 7], as well as non-stationary optical lattices [8–10]. In the latter case counter-propagating laser beams are not perfectly modulated, so they produce an effectively moving optical lattice. An explicit treatment of time-dependent problems is also often required in nuclear and molecular physics [11], and in studies of entanglement phenomena [12–14]. Note that some systems can also be treated effectively as in a time-dependent potential, which actually represents higher nonlinear terms in the wave function. A prominent example is the Gross-Pitaevskii equation, where the nonlinear term is treated within the split-step Crank-Nicolson method as a time-dependent potential which is updated after each time step [15].

A time-dependent formalism has been developed for many theoretical approaches, ranging from such general methods as the time-dependent quantum mechanical perturbation theory to time-dependent variants of highly specialized methods, such as the Density Matrix Renormalization Group (DMRG) [16, 17], the Density Functional Theory (DFT) [18, 19], and the Density Matrix Functional Theory (DMFT) [20]. In numerical approaches, the usual split-operator method, which is based

on a space-grid calculation both without [21, 22] and with Monte-Carlo [23, 24], is mainly used in its second-order variant for time-dependent potentials, where no change is required in comparison with the time-independent case. However, also higher order split-operator schemes have been derived, including fourth [25, 26] and higher-order expansions [27–30].

In this paper, we extend the earlier established approach in Refs. [31–34] for obtaining a high-order short-time expansion of transition amplitudes of time-independent potentials to the important time-dependent case. This development allows a high-precision calculation of transition amplitudes, which is necessary for extracting properties of various quantum systems, such as partition functions. Note that individual transition amplitudes can be accurately calculated using the lower-order effective actions at the expense of increasing the number of Monte Carlo time-steps, which would just increase the needed computation time. Although the presented approach can be used for improving the efficiency for calculating such transition amplitudes, it is mainly developed for applications which require a large number of accurate transition amplitudes for further numerical calculations. Such situations occur, for instance, for determining partition functions [33, 35] or for obtaining energy spectra with the method of diagonalizing the space-discretized evolution operator matrix [36, 37]. In order to avoid an accumulation of numerical errors, so that such calculations can be performed with the required accuracy, the transition amplitudes have to be known more precisely.

Our approach has already been successively used to study global and local properties of rotating Bose-Einstein condensates [38], where the availability of accurately calculated thermal states has allowed to calculate precisely the condensation temperature, the ground-state occupancy, and time-of-flight absorption pictures even in the delicate regime of a critical and an overcritical rotation. If one needs a large numbers of accurate energy eigenvalues and eigenstates, as in this case, higher-order

*E-mail: antun@ipb.ac.rs

[†]Home page: <http://www.scl.rs/>

effective actions become useful. The precise knowledge of the short-time expansion of the propagator might also be used to improve numerical studies of time evolution, especially in systems exhibiting nonlinearities [21], where a time-dependent formalism is required.

Thus, in spirit of Symanzik's improved action programme in quantum field theory [39, 40], we will introduce and analytically derive effective actions for time-dependent potentials which substantially speed up the numerical calculation of transition amplitudes and other quantities for such quantum systems. This approach does not suffer from technical problems related to backwards diffusion in time, as observed and discussed by Sheng [41] and Suzuki [42]. In the split-operator method one has to resort to multiproduct expansions [43] in order to resolve this problem. In the higher-order effective action approach for time-dependent potentials, which is presented here, the convergence of transition amplitudes is always guaranteed in a natural way, as was shown conclusively for the time-independent case in Ref. [44].

The outline of this paper is as follows. In Sec. II we briefly review the underlying path-integral formalism of quantum mechanics [45–48] in order to fix our notation. Afterwards, Sec. III presents a lowest-order path-integral calculation of the short-time transition amplitude for time-dependent potentials in the single-particle one-dimensional case. Based on these lowest-order results, Sec. IV develops the systematic efficient recursive approach for such quantum systems and verifies it numerically with the help of several illustrative one-dimensional models. These recursive calculations to obtain transition amplitudes for time-dependent potentials are then extended to quantum systems with many degrees of freedom in Sec. V. The approach is also numerically verified by using the simple model of a time-dependent multi-component harmonic oscillator system. Furthermore, possible relevant physical applications in the realm of ultracold quantum gases are briefly indicated. Finally, Sec. VI illustrates how the developed imaginary-time formalism is transformed to a real-time one, and demonstrates its applicability by treating several illustrative one-dimensional models.

II. PATH-INTEGRAL FORMALISM

We will consider a non-relativistic quantum multi-component system in d spatial dimensions with a Hamilton operator which consists of the usual kinetic term and a time-dependent potential:

$$\hat{H}(\hat{\mathbf{p}}, \hat{\mathbf{q}}, t) = \sum_{i=1}^P \frac{\hat{\mathbf{p}}_{(i)}^2}{2M_{(i)}} + V(\hat{\mathbf{q}}, t). \quad (1)$$

Here P stands for the number of particles, the $P \times d$ dimensional vectors \mathbf{q} and \mathbf{p} describe positions and momenta of all particles, and the parenthetic subscript (i) denotes the corresponding quantity for particle i . Note

that the potential $V(\mathbf{q}, t)$ is allowed to depend on the positions of all particles, and, therefore, contains implicitly all types of interactions. In practical applications the potential V usually contains, apart from the external potential, also two- and three-body interactions, but further many-body interactions can, in principle, be included as well.

The central object for studying the dynamics of such a quantum system within the path-integral formulation is the transition amplitude

$$A(\mathbf{a}, t_a; \mathbf{b}, t_b) = \langle \mathbf{b}, t_b | \hat{U}(t_a \rightarrow t_b) | \mathbf{a}, t_a \rangle. \quad (2)$$

Here the vectors \mathbf{a} and \mathbf{b} describe the positions of all particles at the initial and final time t_a and t_b , $|\mathbf{a}, t_a\rangle$ and $|\mathbf{b}, t_b\rangle$ denote the corresponding Hilbert-space states of the system, and

$$\hat{U}(t_a \rightarrow t_b) = \hat{T} \exp \left\{ -\frac{i}{\hbar} \int_{t_a}^{t_b} dt \hat{H}(\hat{\mathbf{p}}, \hat{\mathbf{q}}, t) \right\} \quad (3)$$

represents the evolution operator of the system describing its propagation from t_a to t_b . Here we assumed $t_a < t_b$ and introduced the standard time-ordering operator

$$\hat{T}\{\hat{O}(t)\hat{O}(t')\} = \begin{cases} \hat{O}(t)\hat{O}(t'), & \text{if } t > t', \\ \hat{O}(t')\hat{O}(t), & \text{otherwise.} \end{cases} \quad (4)$$

The starting point in setting up the path-integral formalism is the completeness relation

$$A(\mathbf{a}, t_a; \mathbf{b}, t_b) = \int d\mathbf{q}_1 \cdots \int d\mathbf{q}_{N-1} A(\mathbf{a}, t_a; \mathbf{q}_1, t_1) \times A(\mathbf{q}_1, t_1; \mathbf{q}_2, t_2) \cdots A(\mathbf{q}_{N-1}, t_{N-1}; \mathbf{b}, t_b), \quad (5)$$

where $\varepsilon = (t_b - t_a)/N$ denotes the time-slice width, $t_n = t_a + n\varepsilon$ are discrete time steps, and the $P \times d$ dimensional vectors $\mathbf{q}_1, \dots, \mathbf{q}_{N-1}$ describe positions of all particles at a given discrete time step which is specified by the non-parenthetic index. To leading order in ε , the short-time transition amplitude reads

$$A(\mathbf{q}_n, t_n; \mathbf{q}_{n+1}, t_{n+1}) \approx \frac{1}{(2\pi\hbar i\varepsilon)^{Pd/2}} \exp \left\{ \frac{i}{\hbar} S^{(1)}(\mathbf{q}_n, t_n; \mathbf{q}_{n+1}, t_{n+1}) \right\}, \quad (6)$$

where the naive discretized action $S^{(1)}$ is usually expressed as

$$S^{(1)}(\mathbf{q}_n, t_n; \mathbf{q}_{n+1}, t_{n+1}) = \varepsilon \left\{ \frac{1}{2} \left(\frac{\boldsymbol{\delta}_n}{\varepsilon} \right)^2 - V(\mathbf{x}_n, \tau_n) \right\}. \quad (7)$$

Here we introduced the discretized velocity $\boldsymbol{\delta}_n = \mathbf{q}_{n+1} - \mathbf{q}_n$, and rescaled the coordinates so that the mass of all particles is equal to unity. The potential V is evaluated at the mid-point coordinate $\mathbf{x}_n = (\mathbf{q}_n + \mathbf{q}_{n+1})/2$ and at the mid-point time $\tau_n = (t_n + t_{n+1})/2$. Eq. (7) is correct to order $\varepsilon \sim 1/N$ and, therefore, after substitution

to Eq. (6), leads to errors of the order $O(1/N^2)$ for discretized short-time transition amplitudes. Note that the normalization factor $\sim 1/\varepsilon^{Pd/2}$ in Eq. (6) does not affect the N -scaling of errors, since short-time amplitudes will be inserted into the completeness relation (5), where this normalization factor will be added to the normalization of the long-time transition amplitude. However, due to the fact that Eq. (5) contains a product of N short-time transition amplitudes, the deviation of the obtained discrete transition amplitude from the corresponding continuum result will be of the order $N \cdot O(1/N^2) = O(1/N)$. For this reason the naive discretized action is designated by $S^{(1)}$.

In the limit $N \rightarrow \infty$ we recover the continuous transition amplitude, which leads to the formal coordinate-space path-integral expression

$$A(\mathbf{a}, t_a; \mathbf{b}, t_b) = \int_{\mathbf{q}(t_a)=\mathbf{a}}^{\mathbf{q}(t_b)=\mathbf{b}} \mathcal{D}\mathbf{q}(t) \exp \left\{ \frac{i}{\hbar} S[\mathbf{q}] \right\}, \quad (8)$$

where the integration is defined over all possible trajectories $\mathbf{q}(t)$ through the discretization process described above. In this equation, the action S for a given trajectory $\mathbf{q}(t)$ is defined as usual:

$$S[\mathbf{q}] = \int_{t_a}^{t_b} dt \left\{ \frac{1}{2} \dot{\mathbf{q}}^2(t) - V(\mathbf{q}(t), t) \right\}. \quad (9)$$

The outlined derivation represents the basis for the path-integral formulation of quantum mechanics [45–48] as well as for the numerical calculation of path integrals. The described discretization procedure is most straightforwardly numerically implemented by the Path-Integral Monte-Carlo approach [49].

Note that the $O(1/N)$ convergence can be also achieved with other choices of space-time points at which we evaluate the potential in Eq. (7). For example, the left or the right prescription $\mathbf{x}_n = \mathbf{q}_n, \tau_n = t_n$ or $\mathbf{x}_n = \mathbf{q}_{n+1}, \tau_{n+1} = t_{n+1}$ is often used for the spatio-temporal argument of the potential. These different choices do neither affect the numerical calculation nor the analytical derivation, and different prescriptions can even be translated into each other. However, it turns out that the mid-point prescription always yields the simplest analytic results, and, therefore, we will use it throughout the present paper.

In the following we will switch to the imaginary-time formalism, which is widely used in numerical simulations [49], since it mitigates problems which are related to the oscillatory nature of the integrand in the real-time approach. To obtain the real-time from the imaginary-time amplitudes, one would have to perform an inverse Wick-rotation, i.e. a suitable analytic continuation of the numerical results. This might be difficult due to the inherent instability of this procedure with respect to statistical noise, which is always present in numerical calculations. However, using the imaginary time is justified by the fact that all current applications of this approach

are related to quantum statistical physics, which is naturally set up in imaginary time, with the inverse temperature $\beta = 1/k_B T$ playing the role of the imaginary time. Also, energy spectra and energy eigenfunctions can be efficiently calculated in this formalism [36, 37]. Note that the derived analytic expressions for higher-order propagators can be formally transformed from the imaginary- to the real-time axis. As we demonstrate in Sec. VI by treating several simple examples, such analytic expressions can be successfully used for calculating the real-time evolution in the context of the space-discretized approach [36, 37].

After Wick rotation to the imaginary time, the transition amplitude is expressed as

$$A(\mathbf{a}, t_a; \mathbf{b}, t_b) = \int_{\mathbf{q}(t_a)=\mathbf{a}}^{\mathbf{q}(t_b)=\mathbf{b}} \mathcal{D}\mathbf{q}(t) e^{-\frac{1}{\hbar} S_E[\mathbf{q}]}, \quad (10)$$

where the action is replaced by its imaginary-time counterpart, the Euclidean action

$$S_E[\mathbf{q}] = \int_{t_a}^{t_b} dt \left\{ \frac{1}{2} \dot{\mathbf{q}}^2(t) + V(\mathbf{q}(t), t) \right\}, \quad (11)$$

which represents the energy of the system. To simplify the notation, we will drop the subscript E from now on. If we consider in Eq. (10) only diagonal amplitudes, i.e. $\mathbf{a} = \mathbf{b}$, and integrate over \mathbf{a} , we obtain the path-integral expression for the partition function

$$Z(\beta) = \text{Tr} \left\{ \hat{T} \exp \left[-\frac{1}{\hbar} \int_0^{\hbar\beta} dt \hat{H}(t) \right] \right\} \quad (12)$$

by setting $t_a = 0$ and $t_b = \hbar\beta$.

III. PATH-INTEGRAL CALCULATION OF THE PROPAGATOR

In this paper we develop a method for calculating short-time transition amplitudes for time-dependent potentials to high orders in the propagation time. To this end we follow the approach of Ref. [34] and generalize the level $p = 1$ discretized transition amplitude from Eq. (6) in such a way that the exact transition amplitude is written as

$$A(\mathbf{a}, t_a; \mathbf{b}, t_b) = \frac{1}{(2\pi\varepsilon)^{Pd/2}} e^{-S^*(\mathbf{x}, \boldsymbol{\delta}; \varepsilon, \tau)}. \quad (13)$$

Here we use the convention $\hbar = 1$, the ideal discretized effective action reads [44, 50]

$$S^*(\mathbf{x}, \boldsymbol{\delta}; \varepsilon, \tau) = \frac{\boldsymbol{\delta}^2}{2\varepsilon} + \varepsilon W(\mathbf{x}, \boldsymbol{\delta}; \varepsilon, \tau), \quad (14)$$

and W represents the ideal effective potential, which ensures the exactness of the above expression. The latter depends not only on the coordinate mid-point $\mathbf{x} =$

$(\mathbf{a}+\mathbf{b})/2$, the discretized velocity $\delta = \mathbf{b}-\mathbf{a}$, and the time interval $\varepsilon = t_b - t_a$ as already introduced in the case for time-independent potentials, but also on the time midpoint $\tau = (t_a + t_b)/2$, due to the explicit time dependence of the potential.

We will analytically derive a systematic short-time expansion of the effective potential W , which provides an improved convergence for numerically calculating transition amplitudes and partition functions as well as other properties of quantum systems with time-dependent potentials. The expansion of the effective potential W to order ε^{p-1} yields the effective action correct to order ε^p , with errors proportional to ε^{p+1} . Due to the normalization factor in the expression (13), the total ε -convergence of the amplitude is given by

$$A_p(\mathbf{a}, t_a; \mathbf{b}, t_b) = A(\mathbf{a}, t_a; \mathbf{b}, t_b) + O(\varepsilon^{p+1-Pd/2}). \quad (15)$$

This ε -scaling of errors is valid if we are interested in calculating short-time transition amplitudes, which is the main objective of this paper. However, if we use such short-time transition amplitudes to calculate long-time transition amplitudes through the time-discretization procedure (5), the normalization factors will be again added, and we will get total errors of the order $N \cdot O(1/N^{p+1}) = O(1/N^p)$. Although the corresponding effective actions and resulting discretized short-time transition amplitudes are designated by the index p according to their N -scaling behavior, we stress that the scaling with respect to the short propagation time is always given by Eq. (15).

Before we embark upon developing a systematic recursive approach for analytically calculating higher-order effective actions, we first have to study the general structure of the effective potential, which turns out to be more complex than in the case of time-independent quantum systems. In order to do so, we calculate the short-time expansion of the effective potential by using an *ab initio* approach introduced in Ref. [33]. To simplify the calculation, we will restrict ourselves in the present section to the single-particle one-dimensional case. Based on these results we will develop in Sec. IV the systematic recursive approach for such simple quantum systems, and then extend and generalize this procedure to systems with many degrees of freedom.

Following Ref. [33], we start with changing the variables via $q(t) = \xi(t) + y(t)$, where $\xi(t)$ is some chosen reference trajectory satisfying the same boundary conditions as the path $q(t)$, i.e. $\xi(t_a) = a$, $\xi(t_b) = b$. This implies that the new variable $y(t)$ vanishes at the boundaries, i.e. $y(t_a) = y(t_b) = 0$. We also introduce a new time variable s by $t = \tau + s$, in which the boundaries are defined by $s_a = -\varepsilon/2$, $s_b = \varepsilon/2$. In the new variables, the kinetic energy functional has the form

$$\begin{aligned} & \int_{t_a}^{t_b} dt \frac{1}{2} \left(\frac{dq(t)}{dt} \right)^2 \\ &= \int_{-\varepsilon/2}^{\varepsilon/2} ds \left\{ \frac{1}{2} \dot{\xi}^2(s) + \frac{1}{2} \dot{y}^2(s) - y(s) \ddot{\xi}(s) \right\}, \quad (16) \end{aligned}$$

where a dot represents a derivative with respect to the time s . With this the transition amplitude reads

$$\begin{aligned} A(a, t_a; b, t_b) &= e^{-S[\xi](\tau)} \int_{y(-\varepsilon/2)=0}^{y(\varepsilon/2)=0} \mathcal{D}y(s) \\ &\times e^{-\int_{-\varepsilon/2}^{\varepsilon/2} ds \left\{ \frac{1}{2} \dot{y}^2(s) + U_\xi(y(s), s) \right\}}, \quad (17) \end{aligned}$$

where the quantity U_ξ is defined as

$$U_\xi(y(s), s) = V(\xi(s) + y(s), \tau + s) - V(\xi(s), \tau) - y(s) \ddot{\xi}(s), \quad (18)$$

and the Euclidean action $S[\xi](\tau)$ for the reference trajectory $\xi(s)$ is defined by an expression similar to Eq. (11), but with the time argument of the potential being fixed now by the midpoint τ :

$$S[\xi](\tau) = \int_{-\varepsilon/2}^{\varepsilon/2} ds \left\{ \frac{1}{2} \dot{\xi}^2(s) + V(\xi(s), \tau) \right\}. \quad (19)$$

Thus, the transition amplitude reads

$$A(a, t_a; b, t_b) = \frac{e^{-S[\xi](\tau)}}{\sqrt{2\pi\varepsilon}} \left\langle e^{-\int_{-\varepsilon/2}^{\varepsilon/2} ds U_\xi(y(s), s)} \right\rangle, \quad (20)$$

where the path-integral expectation value is defined with respect to the free-particle action:

$$\langle \bullet \rangle = \sqrt{2\pi\varepsilon} \int_{y(-\varepsilon/2)=0}^{y(\varepsilon/2)=0} \mathcal{D}y(s) \bullet e^{-\int_{-\varepsilon/2}^{\varepsilon/2} ds \frac{1}{2} \dot{y}^2(s)}. \quad (21)$$

The transition amplitude (20) can then be obtained through a standard calculation of the free-particle expectation value by using the Taylor expansion

$$\begin{aligned} \left\langle e^{-\int_{-\varepsilon/2}^{\varepsilon/2} ds U_\xi(y(s), s)} \right\rangle &= 1 - \int_{-\varepsilon/2}^{\varepsilon/2} ds \langle U_\xi(y(s), s) \rangle \\ &+ \frac{1}{2} \int_{-\varepsilon/2}^{\varepsilon/2} ds \int_{-\varepsilon/2}^{\varepsilon/2} ds' \langle U_\xi(y(s), s) U_\xi(y(s'), s') \rangle + \dots \end{aligned} \quad (22)$$

As we see from Eq. (18), the quantity U_ξ has the simplest form if we choose the reference trajectory ξ in such a way that its second derivative with respect to the time s vanishes. The natural choice is thus the linear trajectory $\xi(s) = x + s\delta/\varepsilon$, centered around the midpoint $x = (a+b)/2$. In order to calculate the expectation values in Eq. (22), we further have to expand

$$U_\xi(y(s), s) = V(\xi(s) + y(s), \tau + s) - V(\xi(s), \tau) \quad (23)$$

around this reference trajectory according to

$$U_\xi(y(s), s) = \sum_{\substack{n, m \\ n+m > 0}} \frac{1}{n! m!} {}^{(m)}V^{(n)}(\xi(s), \tau) y^n(s) s^m, \quad (24)$$

where (m) denotes the order of the derivative with respect to the time s , and (n) denotes the order of spatial derivatives. For a free-particle theory, expectation values

of the type $\langle y^{n_1}(s_1) y^{n_2}(s_2) \dots \rangle$ can be easily calculated using the standard generating functional approach. The expectation value $\langle y(s) \rangle$ vanishes due to the symmetry, while the correlator $\Delta(s, s') = \langle y(s) y(s') \rangle$ is given by the expression

$$\Delta(s, s') = \frac{\theta(s - s')}{\varepsilon} \left(\frac{\varepsilon}{2} - s \right) \left(\frac{\varepsilon}{2} + s' \right) + (s \leftrightarrow s'), \quad (25)$$

and higher expectation values can be found in Ref. [33].

In order to obtain an expansion of the transition amplitude in the propagation time ε , one has to consider Eq. (22) and to take into account the powers of ε of all terms to identify the relevant terms at the desired level p . To illustrate this, let us look at the term linear in U_ξ

$$\begin{aligned} & \int_{-\varepsilon/2}^{\varepsilon/2} ds \langle U_\xi(y(s), s) \rangle \\ &= \int_{-\varepsilon/2}^{\varepsilon/2} ds \sum_{\substack{n, m \\ n+m > 0}} \frac{1}{n! m!} V^{(n)}(\xi(s), \tau) \langle y^n(s) \rangle s^m, \end{aligned} \quad (26)$$

$$\begin{aligned} \left\langle e^{-\int_{-\varepsilon/2}^{\varepsilon/2} ds U_\xi(y(s), s)} \right\rangle &= 1 - \int_{-\varepsilon/2}^{\varepsilon/2} ds \left\{ \frac{1}{2} V''(\xi(s), \tau) \langle y^2(s) \rangle + \frac{1}{24} V^{(4)}(\xi(s), \tau) \langle y^4(s) \rangle + \dot{V}(\xi(s), \tau) s \right. \\ &\quad \left. + \frac{1}{2} \dot{V}^{(2)}(\xi(s), \tau) \langle y^2(s) \rangle s + \frac{1}{2} \ddot{V}(\xi(s), \tau) s^2 \right\} + \frac{1}{2} \int_{-\varepsilon/2}^{\varepsilon/2} ds \int_{-\varepsilon/2}^{\varepsilon/2} ds' V'(\xi(s), \tau) V'(\xi(s'), \tau) \langle y(s) y(s') \rangle + O(\varepsilon^4). \end{aligned} \quad (27)$$

In the above expression, the correlators $\langle y^2(s) \rangle = \Delta(s, s)$ and $\langle y(s) y(s') \rangle = \Delta(s, s')$ are given by Eq. (25), and the expectation value $\langle y^4(s) \rangle$ can be directly determined using either the generating functional method or the Wick rule, yielding $3\Delta^2(s, s)$. In order to be able to calculate the remaining integrals over s and s' , we need to expand also the potential V and its derivatives with respect to the first argument $\xi(s) = x + s\delta/\varepsilon$ around the mid-point x . The required number of terms in this expansion, contributing to the desired order of ε , is obtained by taking into account the diffusion relation $\delta^2 \sim \varepsilon$, which is valid for small propagation times ε and has been demonstrated to yield a consistent expansion of short-time transition amplitudes [34]. The expansion of the potential into power series in $s\delta/\varepsilon$ gives an additional polynomial s -dependence, which finally allows an analytic calculation of all integrals in Eq. (27). When this is done, we obtain the following expression for the expectation value (22)

$$\begin{aligned} \left\langle e^{-\int_{-\varepsilon/2}^{\varepsilon/2} ds U_\xi(y(s), s)} \right\rangle &= 1 - V'' \frac{\varepsilon^2}{12} - \dot{V}' \frac{\delta \varepsilon^2}{12} \\ &\quad - V^{(4)} \frac{\varepsilon^3}{240} - \ddot{V} \frac{\varepsilon^3}{24} + V'^2 \frac{\varepsilon^3}{24} - V^{(4)} \frac{\delta^2 \varepsilon^2}{480} \\ &\quad - \dot{V}^{(3)} \frac{\delta \varepsilon^3}{240} - \dot{V}^{(3)} \frac{\delta^3 \varepsilon^2}{480} + O(\varepsilon^4), \end{aligned} \quad (28)$$

where the potential V as well as its spatial and tem-

poral derivatives are evaluated at the mid-point x, τ , i.e. $V = V(x, \tau)$. Note that we have retained in Eq. (28) only those terms whose order is less than ε^4 . Taking into account the diffusion relation $\delta^2 \sim \varepsilon$, the terms proportional to ε^3 and $\delta^2 \varepsilon^2$ are considered to be of the same order.

Combining Eqs. (13) and (20), we see that the ideal effective action can be expressed by its short-time expression (19) and the expectation value (22) according to

$$S^*(x, \delta; \varepsilon, \tau) = S[\xi](\tau) - \log \left\langle e^{-\int_{-\varepsilon/2}^{\varepsilon/2} ds U_\xi(y(s), s)} \right\rangle. \quad (29)$$

After expanding the potential V around the mid-point x in the action $S[\xi](\tau)$ in Eq. (19), we obtain its short-time expansion:

$$S[\xi](\tau) = \frac{\delta^2}{2\varepsilon} + V\varepsilon + V'' \frac{\delta^2 \varepsilon}{24} + V^{(4)} \frac{\delta^4 \varepsilon}{1920} + O(\varepsilon^4). \quad (30)$$

This allows us to calculate the short-time expansion of the effective potential W from Eqs. (14) and (28)–(30). For example, up to level $p = 3$ we get

$$\begin{aligned} W_3(x, \delta; \varepsilon, \tau) &= V + V'' \frac{\varepsilon}{12} + V'' \frac{\delta^2}{24} + \dot{V}' \frac{\delta \varepsilon}{12} \\ &\quad + V^{(4)} \frac{\varepsilon^2}{240} + \ddot{V} \frac{\varepsilon^2}{24} - V'^2 \frac{\varepsilon^2}{24} + V^{(4)} \frac{\delta^2 \varepsilon}{480} + V^{(4)} \frac{\delta^4}{1920}. \end{aligned} \quad (31)$$

Numerically, such a result allows to speed up the calculation of transition amplitudes, since the errors can be substantially reduced using analytic expressions for higher level effective actions.

Compared to our previous results for effective actions of time-independent potentials V in Ref. [34], we see that new terms appear which contain time derivatives of the potential. In particular, we observe the emergence of terms with odd powers of the discretized velocity δ , which was previously not the case. In fact, for time-independent potentials we have shown in Ref. [34] that the effective potential is symmetric in δ , which leaves only even powers of δ in its short-time expansion. Here, however, also odd powers of δ survive due to the explicit time dependence of the potential. We also recognize that all new terms are proportional to time derivatives of the potential and vanish in the time-independent case, thus reducing the effective action to the previous expressions in Ref. [34].

Therefore, the correct systematic short-time expansion of the effective potential turns out to have the form

$$W(x, \delta; \varepsilon, \tau) = \sum_{m=0}^{\infty} \sum_{k=0}^m \left\{ c_{m,k}(x, \tau) \varepsilon^{m-k} \left(\frac{\delta}{2} \right)^{2k} + c_{m+1/2,k}(x, \tau) \varepsilon^{m-k} \left(\frac{\delta}{2} \right)^{2k+1} \right\}. \quad (32)$$

Here $\delta/2$ is used as the expansion parameter in order to have expansion coefficients c which are defined consistently with Ref. [34]. Such an expansion allows that the level p effective action is written as the sum of terms corresponding to $m = 0, 1, \dots, p-1$. Note that for $m = p-1$ we need to take into account only the even-power terms $c_{p-1,k}(x, \tau) \varepsilon^{p-1-k} (\delta/2)^{2k}$. The odd-power terms $c_{p-1/2,k}(x, \tau) \varepsilon^{p-1-k} (\delta/2)^{2k+1}$ are proportional to $\varepsilon^{p-1/2}$, i.e. they are of higher order than the required ε^{p-1} for level p effective action. For this reason, the correct expansion of the effective potential at level p is given by

$$W_p(x, \delta; \varepsilon, \tau) = \sum_{m=0}^{p-1} \sum_{k=0}^m c_{m,k}(x, \tau) \varepsilon^{m-k} \left(\frac{\delta}{2} \right)^{2k} + \sum_{m=0}^{p-2} \sum_{k=0}^m c_{m+1/2,k}(x, \tau) \varepsilon^{m-k} \left(\frac{\delta}{2} \right)^{2k+1}, \quad (33)$$

and it provides the convergence of transition amplitudes according to Eq. (15).

IV. RECURSIVE CALCULATION OF THE PROPAGATOR

In this section we will use the latter result (32) to develop a systematic recursive approach for analytically calculating effective actions to high levels p for time-dependent potentials. To this end we rederive at first both the forward and the backward Schrödinger equation

for the transition amplitude and then use them to derive corresponding differential equations for the effective potential W . Afterwards, we use Eq. (32) to solve them and obtain recursion relations, first for a simple single-particle one-dimensional potential and, subsequently in Sec. V, for a general quantum system with many degrees of freedom. The obtained analytical results are illustrated and verified by numerical Monte-Carlo simulations which are performed for several simple models.

A. Forward and Backward Schrödinger Equation

The evolution operator for quantum system in a time-dependent potential is given by Eq. (3), or, in imaginary time,

$$\hat{U}(t_a \rightarrow t_b) = \hat{T} \exp \left\{ - \int_{t_a}^{t_b} dt \hat{H}(\hat{\mathbf{p}}, \hat{\mathbf{q}}, t) \right\}. \quad (34)$$

Thus, the evolution operator obeys the differential equation

$$\partial_{t_b} \hat{U}(t_a \rightarrow t_b) = -\hat{H}(\hat{\mathbf{p}}, \hat{\mathbf{q}}, t_b) \hat{U}(t_a \rightarrow t_b), \quad (35)$$

and, similarly,

$$\partial_{t_a} \hat{U}(t_a \rightarrow t_b) = \hat{U}(t_a \rightarrow t_b) \hat{H}(\hat{\mathbf{p}}, \hat{\mathbf{q}}, t_a). \quad (36)$$

If we determine from Eq. (35) the matrix elements which correspond to the transition amplitude Eq. (2), we obtain the forward Schrödinger equation for the transition amplitude

$$\partial_{t_b} A(\mathbf{a}, t_a; \mathbf{b}, t_b) = -\hat{H}_b A(\mathbf{a}, t_a; \mathbf{b}, t_b), \quad (37)$$

where \hat{H}_b stands for the coordinate-space Hamilton operator $\hat{H}_b = H(-i\partial_{\mathbf{b}}, \mathbf{b}, t_b)$, in which momentum and position operators are replaced by their coordinate-space representations at \mathbf{b} . To obtain the analogous equation for the derivative with respect to the initial time t_a , we have to take into account that the imaginary-time transition amplitudes as well as its time derivative are real. With this Eq. (36) yields at first

$$\begin{aligned} \langle \mathbf{b} | \partial_{t_a} \hat{U}(t_a \rightarrow t_b) | \mathbf{a} \rangle \\ = H(-i\partial_{\mathbf{a}}, \mathbf{a}, t_a) \langle \mathbf{a} | \hat{U}^\dagger(t_a \rightarrow t_b) | \mathbf{b} \rangle. \end{aligned} \quad (38)$$

Since we have in addition

$$\langle \mathbf{a} | \hat{U}^\dagger(t_a \rightarrow t_b) | \mathbf{b} \rangle = A(\mathbf{a}, t_a; \mathbf{b}, t_b), \quad (39)$$

we finally get the backward Schrödinger equation for the transition amplitude

$$\partial_{t_a} A(\mathbf{a}, t_a; \mathbf{b}, t_b) = \hat{H}_a A(\mathbf{a}, t_a; \mathbf{b}, t_b), \quad (40)$$

where $\hat{H}_a = H(-i\partial_{\mathbf{a}}, \mathbf{a}, t_a)$ is defined analogously as \hat{H}_b .

In the next step we change the original time variables t_a and t_b to the mid-point τ and the propagation time ε , which converts (37) and (40) to

$$\left[\partial_\varepsilon + \frac{1}{2}(\hat{H}_a + \hat{H}_b) \right] A(\mathbf{a}, t_a; \mathbf{b}, t_b) = 0, \quad (41)$$

$$\left[\partial_\tau + (\hat{H}_b - \hat{H}_a) \right] A(\mathbf{a}, t_a; \mathbf{b}, t_b) = 0. \quad (42)$$

Subsequently, we also change the spatial variables \mathbf{a} and \mathbf{b} to the mid-point \mathbf{x} and the discretized velocity $\bar{\mathbf{x}} = \delta/2$, thus Eqs. (41) and (42) read then

$$\left[\partial_\varepsilon - \frac{1}{8} \partial^2 - \frac{1}{8} \bar{\partial}^2 + \frac{1}{2} (V_+ + V_-) \right] A(\mathbf{x}, \bar{\mathbf{x}}; \varepsilon, \tau) = 0, \quad (43)$$

$$\left[\partial_\tau - \frac{1}{2} \partial \bar{\partial} + V_+ - V_- \right] A(\mathbf{x}, \bar{\mathbf{x}}; \varepsilon, \tau) = 0, \quad (44)$$

where we have introduced $V_\pm = V(\mathbf{x} \pm \bar{\mathbf{x}}, \tau \pm \frac{\varepsilon}{2})$ as abbreviations, and the $P \times d$ -dimensional Laplacians $\partial_{\mathbf{x}} \cdot \partial_{\mathbf{x}} = \partial^2$ over coordinates \mathbf{x} and $\partial_{\bar{\mathbf{x}}} \cdot \partial_{\bar{\mathbf{x}}} = \bar{\partial}^2$ over coordinates $\bar{\mathbf{x}}$, as well as the mixed Laplacian $\partial_{\mathbf{x}} \cdot \partial_{\bar{\mathbf{x}}} = \partial \bar{\partial}$. Note that we will not use Eq. (44) in our further calculation of the short-time transition amplitude. This equation describes the dynamics caused only by the presence of the explicit time-dependence of the potential, as is indicated by the derivative with respect to the time mid-point τ .

If we now express the transition amplitude (13) by using the effective potential in (14) and the new spatio-temporal variables, we get

$$A(\mathbf{x}, \bar{\mathbf{x}}; \varepsilon, \tau) = \frac{1}{(2\pi\varepsilon)^{Pd/2}} e^{-\frac{2}{\varepsilon} \bar{\mathbf{x}}^2 - \varepsilon W(\mathbf{x}, \bar{\mathbf{x}}; \varepsilon, \tau)}. \quad (45)$$

Substituting this expression into the differential equation for the transition amplitude (43), we obtain a corresponding differential equation for the effective potential:

$$W + \bar{\mathbf{x}} \cdot \bar{\partial} W + \varepsilon \partial_\varepsilon W - \frac{1}{8} \varepsilon \partial^2 W - \frac{1}{8} \varepsilon \bar{\partial}^2 W + \frac{1}{8} \varepsilon^2 (\partial W)^2 + \frac{1}{8} \varepsilon^2 (\bar{\partial} W)^2 = \frac{1}{2} (V_+ + V_-). \quad (46)$$

This equation is formally identical to the corresponding equation (29) from Ref. [34], and in the limit of the time-independent potential we recover the previously derived result. Eq. (46) can now be used to develop a recursive approach for calculating the effective potential W by using the double power series (32) in both ε and $\bar{\mathbf{x}}$.

B. Single-Particle One-Dimensional Systems

Before we deal with the general case, we will first consider a single-particle one-dimensional system in a given external time-dependent potential V . The right-hand side of Eq. (46) can then be expanded in a double power series of the form

$$\begin{aligned} & \frac{1}{2} (V_+ + V_-) \\ &= \frac{1}{2} \sum_{k, m \geq 0} \frac{1}{k! m!} V^{(m)} V^{(k)} \left(\frac{\varepsilon}{2} \right)^m \bar{x}^k \left\{ 1 + (-1)^{m+k} \right\}. \end{aligned} \quad (47)$$

We see that m and k must be of the same parity in order to yield a non-zero contribution. Therefore, we introduce the quantity $\Pi(m, k)$, which is equal to one if $m - k$ is even, and vanishes otherwise. This allows us to reorganize terms of the double power series (48) in a form which corresponds to the expansion of the effective potential in Eq. (32):

$$\begin{aligned} \frac{1}{2} (V_+ + V_-) &= \sum_{m=0}^{\infty} \sum_{k=0}^m \left\{ \frac{\Pi(m, k) \varepsilon^{m-k} \bar{x}^{2k}}{(2k)! (m-k)! 2^{m-k}} V^{(m-k)} V^{(2k)} \right. \\ &\quad \left. + \frac{[1 - \Pi(m, k)] \varepsilon^{m-k} \bar{x}^{2k+1}}{(2k+1)! (m-k)! 2^{m-k}} V^{(m-k)} V^{(2k+1)} \right\}. \end{aligned} \quad (48)$$

In order to solve Eq. (46) with (48), we now substitute the effective potential W with its double expansion (32). By comparing terms with even and odd powers of \bar{x} , we obtain algebraic equations which determine the coefficients $c_{m,k}$ and $c_{m+1/2,k}$. After a straight-forward calculation we get

$$\begin{aligned} 8(m+k+1) c_{m,k} &= 8 \frac{\Pi(m, k) V^{(m-k)} V^{(2k)}}{(2k)! (m-k)! 2^{m-k}} + (2k+2)(2k+1) c_{m,k+1} + c_{m-1,k}'' - \sum_{l,r} \left\{ c_{l,r}' c_{m-l-2,k-r}' \right. \\ &\quad \left. + c_{l+1/2,r}' c_{m-l-5/2,k-r-1}' + 2r(2k-2r+2) c_{l,r} c_{m-l-1,k-r+1} + (2r+1)(2k-2r+1) c_{l+1/2,r} c_{m-l-3/2,k-r} \right\}, \end{aligned} \quad (49)$$

$$\begin{aligned} 8(m+k+2) c_{m+1/2,k} &= 8 \frac{[1 - \Pi(m, k)] V^{(m-k)} V^{(2k+1)}}{(2k+1)! (m-k)! 2^{m-k}} + (2k+3)(2k+2) c_{m+1/2,k+1} + c_{m-1/2,k}'' - \sum_{l,r} \left\{ c_{l,r}' c_{m-l-3/2,k-r}' \right. \\ &\quad \left. + c_{l+1/2,r}' c_{m-l-2,k-r}' + (2r+1)(2k-2r+2) c_{l+1/2,r} c_{m-l-1,k-r+1} + 2r(2k-2r+3) c_{l,r} c_{m-l-1/2,k-r+1} \right\}. \end{aligned} \quad (50)$$

In the above relations, sums over l and r are restricted by the non-negativity of indices for both even and odd-

power coefficients c . It is immediately seen in the case

of a time-independent potential that the recursion for even-power coefficients $c_{m,k}$ in Eq. (49) reduces to the previously derived recursion of Ref. [34], while the odd-power recursion (50) automatically renders all coefficients $c_{m+1/2,k}$ to be zero.

In order to efficiently solve these algebraic equations at a given level p , we recall the corresponding hierarchical level p expansion (33). In such an expansion, we look only for even-power coefficients $c_{m,k}$ with $0 \leq m \leq p-1$, and odd-power coefficients $c_{m+1/2,k}$ with $0 \leq m \leq p-2$, while the index k is always restricted by $0 \leq k \leq m$. To simplify the calculation, we formally set all the coefficients with higher values of indices to zero. As in case for a time-independent potential in Ref. [34], we are then able to calculate explicitly diagonal even-order coefficient $c_{m,m}$ for any m :

$$c_{m,m} = \frac{V^{(2m)}}{(2m+1)!}. \quad (51)$$

Correspondingly, we obtain for the diagonal odd-power coefficients the general result

$$c_{m+1/2,m} = 0. \quad (52)$$

Thus, the recursion relations (49) and (50) represent together with (51) and (52) a closed set of algebraic equations, which completely determines the coefficients c for the effective potential at a given level p .

To illustrate how the recursive procedure works in detail, we solve the single-particle recursive relations up to order $p = 3$ and demonstrate that we obtain the same result (31) as in the previous section, where we used the path-integral approach to calculate the effective potential. For the level $p = 3$ we need coefficients c with the first index m in the range $0, \dots, p-1$, i.e. $m = 0, 1, 2$. For a given $m \leq p-1$ we start with calculating even-power coefficients $c_{m,k}$ by using the recursive relation (49) in the order $k = m, m-1, \dots, 0$, where we take into account (51). Then we proceed with the calculation of odd-power coefficients $c_{m+1/2,k}$ by using Eq. (50) for the order $k = m-1, \dots, 0$ and by taking into account (52). We also recall that odd-power coefficients need not be calculated for $m = p-1$, i.e. in the last step of the recursive procedure for $m = p-1$ we only calculate even-power coefficients. Following this procedure, we immediately from get (51) for $m = 0$

$$c_{0,0} = V. \quad (53)$$

The coefficient $c_{1/2,0} = 0$ follows trivial from (52). For $m = 1$ we get the following even-power coefficients, corresponding to the values $k = 1$ and $k = 0$:

$$c_{1,1} = \frac{1}{6}V'', \quad (54)$$

$$c_{1,0} = \frac{1}{16}c''_{0,0} + \frac{1}{8}c_{1,1} = \frac{1}{12}V''. \quad (55)$$

For the only non-trivial $m = 1$ odd-power coefficient $c_{3/2,0}$ we get

$$c_{3/2,0} = \frac{1}{4}c_{3/2,1} + \frac{1}{24}c''_{1/2,0} + \frac{1}{6}\dot{V}' = \frac{1}{6}\dot{V}'. \quad (56)$$

Similarly, we find the $m = 2$ even-power coefficients by using Eqs. (49) and (51):

$$c_{2,2} = \frac{1}{120}V^{(4)}, \quad (57)$$

$$c_{2,1} = \frac{1}{32}c''_{1,1} + \frac{3}{8}c_{2,2} = \frac{1}{120}V^{(4)}, \quad (58)$$

$$\begin{aligned} c_{2,0} &= \frac{1}{24}\ddot{V} - \frac{1}{24}c''_{0,0} + \frac{1}{24}c''_{1,0} + \frac{1}{12}c_{2,1} \\ &= \frac{1}{24}\ddot{V} + \frac{V^{(4)}}{240} - \frac{V'^2}{24}. \end{aligned} \quad (59)$$

This result is already sufficient to construct the effective potential $W_{p=3}$. If we insert the calculated coefficients in the expansion (33) at the given level $p = 3$, we reobtain the same expression as in Eq. (31). Comparing the calculated even-power coefficients $c_{m,k}$ with the previously calculated ones for the time-independent potential in Ref. [34], we see that they coincide if we set all time derivatives of the potential to zero, as expected, and that all odd-power coefficients vanish.

We stress that the recursive approach is far more efficient than the path-integral calculation presented in the previous section. For example, if one wants to extend a level p calculation to a higher order $p' = p+1$, this requires in the path-integral approach not only to take into account the next term in the expansion (27), but also each previously calculated expectation value term has to be redone to one order in ε higher. The complexity of this algorithm prevents its efficient implementation. However, in the present recursive approach, all we need to do is to calculate one additional order of odd-power coefficients $c_{p-1/2,k}$, which corresponds to $m = p' - 2 = p - 1$, and even-power coefficients $c_{p,k}$, which corresponds to $m = p' - 1 = p$. To do this, we just apply the recursive relations and use previously calculated lower-order coefficients c . For instance, in order to obtain level $p' = 4$, we proceed first with calculating $m = p' - 2 = 2$ odd-power coefficients $c_{5/2,k}$. The highest coefficient $c_{5/2,2} = 0$ is automatically equal to zero due to (52), while for lower-level coefficients we get

$$c_{5/2,1} = \frac{1}{2}c_{5/2,2} + \frac{1}{40}c''_{3/2,1} + \frac{1}{60}\dot{V}^{(3)} = \frac{1}{60}\dot{V}^{(3)}, \quad (60)$$

$$\begin{aligned} c_{5/2,0} &= \frac{3}{16}c_{5/2,1} + \frac{1}{32}c''_{3/2,0} - \frac{1}{16}c'_{1/2,0}c'_{0,0} \\ &\quad - \frac{1}{8}c_{1/2,0}c_{1,1} = \frac{1}{120}\dot{V}^{(3)}. \end{aligned} \quad (61)$$

To completely determine the $p' = 4$ effective action, we then calculate even-power $m = p' - 1 = 3$ coefficients

$c_{3,k}$, and obtain from Eqs. (49) and (51)

$$c_{3,3} = \frac{1}{5040} V^{(6)}, \quad (62)$$

$$c_{3,2} = \frac{1}{3360} V^{(6)}, \quad (63)$$

$$c_{3,1} = \frac{1}{3360} V^{(6)} + \frac{1}{80} \ddot{V}'' - \frac{1}{360} V''^2 - \frac{1}{120} V' V^{(3)}, \quad (64)$$

$$c_{3,0} = \frac{1}{6720} V^{(6)} + \frac{1}{480} \ddot{V}'' - \frac{1}{360} V''^2 - \frac{1}{120} V' V^{(3)}. \quad (65)$$

The outlined procedure continues in the same way for higher levels p . We have automatized this procedure and implemented it using the Mathematica 7.0 package [51] for symbolic calculus. Using this we have determined the effective action for a one-dimensional particle in a general time-dependent potential up to the level $p = 20$. Such calculation requires around 2 GB of memory and approximately 1.5 hours of CPU time on 2.33 GHz Intel Xeon E5345 processor. Although the effective actions grow in complexity with level p , the Schrödinger equation method for calculating the discrete-time effective actions turns out to be extremely efficient. The value of $p = 20$ far surpasses the previously obtained best result known in literature of $p = 6$ [29], and is limited practically only by the sheer size of the expression for the effective action of a general theory at such a high level. The whole technique can be pushed even much further when working on specific potential classes as, for instance, polynomial potentials, where higher spatial and temporal derivatives have a simple form. However, if this is not the case, the obtained general expressions for the effective potential can be used for any given potential.

In practical applications, the increasing complexity of expressions for higher-level effective actions leads to a corresponding increase in the necessary computation time. For levels $p \lesssim 10$ [31, 32], the increase in the computation time is minimal compared to the obtained decrease in the error of numerically calculated transition amplitudes, thus it can be used to speed up the calculation at a given level of accuracy. However, for higher values of p the error may be more efficiently reduced by decreasing the time step, i.e. by using a larger number of Monte Carlo discretization steps. Since the complexity of effective actions strongly depends on the concrete form of the given potential, the optimal values of both the level p and the size of the time step have to be estimated from a series of scaled-down numerical simulations. For example, level $p = 21$ and a certain time step have turned out to be optimal for studying fast-rotating Bose-Einstein condensates in an anharmonic trapping potential [38].

C. Test Models

In order to numerically verify the derived analytical results, we have studied several simple models with time-dependent potentials. We have used the modified version

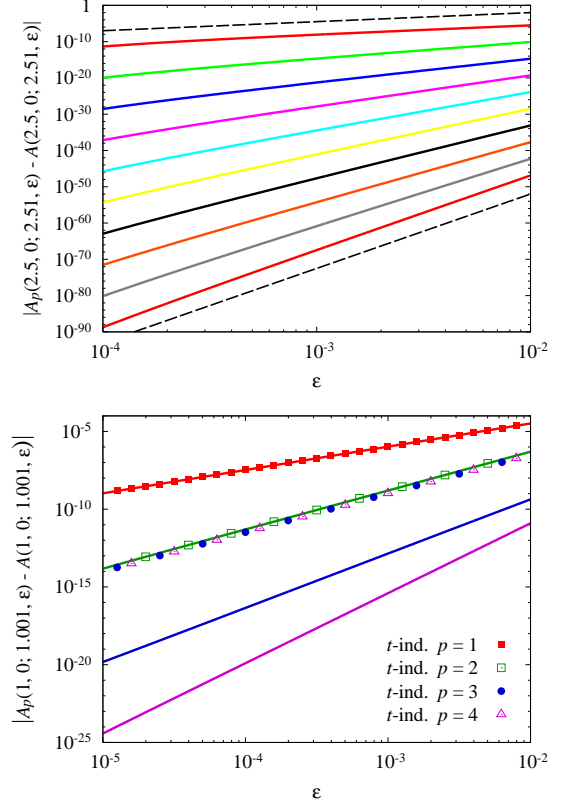


FIG. 1: (Color online) Deviations of amplitudes as functions of propagation time $\varepsilon = t_b - t_a$ for the harmonic oscillator (67), rescaled with the Grosche factor $\zeta(t) = \sqrt{t^2 + 1}$. (top) Deviations of amplitudes $|A_p(2.5, 0; 2.51, \varepsilon) - A(2.5, 0; 2.51, \varepsilon)|$ as functions of ε , calculated analytically for $p = 2, 4, 6, 8, 10, 12, 14, 16, 18, 20$ from top to bottom. The dashed lines are proportional to $\varepsilon^{2.5}$ and $\varepsilon^{20.5}$ and demonstrate the perfect scaling of the corresponding level $p = 2$ and $p = 20$ results. (bottom) Comparison of deviations $|A_p(1, 0; 1.001, \varepsilon) - A(1, 0; 1.001, \varepsilon)|$ calculated using the correct level $p = 1, 2, 3, 4$ effective potentials (full lines, top to bottom) with the deviations obtained for the same levels p of previously derived effective actions [34] for the case of time-independent potential. Deviations for different levels p of time-independent effective actions correspond to different point types.

of the Monte-Carlo SPEEDUP [52] code, which implements higher order effective actions in the C programming language. In order to be able to resolve decreasingly small errors associated with higher levels p of the effective potential, we decided to consider at first some exactly solvable potentials.

In Ref. [53] it was shown that a generalized Duru-Kleinert transformation [48, 54, 55] allows to map the transition amplitude for a time-independent potential $V(x)$ to the corresponding transition amplitude for the time-dependent potential

$$V_G(x, t) = \frac{1}{\zeta^2(t)} V\left(\frac{x}{\zeta(t)}\right), \quad (66)$$

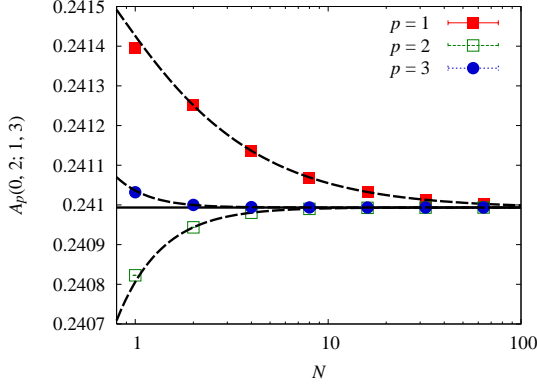


FIG. 2: (Color online) Convergence of numerical Monte-Carlo results for the transition amplitude $A_p(0, 2; 1, 3)$ as a function of the number of time steps N for the time-dependent harmonic oscillator (67), calculated with level $p = 1, 2, 3$ effective actions. The dashed lines give the fitted functions $A_p + B_p/N^p + \dots$, where the constant term A_p corresponds to the continuum-theory amplitude $A_p(0, 2; 1, 3)$. The number of Monte-Carlo samples was $N_{\text{MC}} = 2 \cdot 10^9$.

where $\zeta^2(t) = \zeta_0 + \zeta_1 t + \zeta_2 t^2$ is a general quadratic polynomial in time. Fig. 1 presents the numerical results for the time-dependent harmonic oscillator potential, where the time dependence is introduced by using the Grosche rescaling factor $\zeta(t) = \sqrt{1 + t^2}$:

$$V_{\text{G,HO}}(x, t) = \frac{\omega^2 x^2}{2(1 + t^2)^2}. \quad (67)$$

In the top plot of Fig. 1 we see that the obtained discretized amplitudes converge to the continuum limit systematically faster and faster when we use higher level effective actions. This log-log plot demonstrates that the analytically derived law $\varepsilon^{p+1/2}$ for deviations of single-particle discretized transition amplitudes in $d = 1$ from the continuum transition amplitudes holds perfectly, which verifies numerically our analytical results. The deviations are calculated using the analytically known continuous transition amplitude [53]. The bottom graph of Fig. 1 illustrates the importance of terms with time derivatives of the potential in higher-order effective actions. In this plot we show deviations of discretized transition amplitudes calculated using the effective actions for time-independent potentials, derived in Ref. [34], and compare them with the deviations of discretized transition amplitudes calculated with the correct effective actions, derived here for the case of time-dependent potentials. As can be seen from the graph, time-independent effective actions do not improve results after level $p = 2$, due to the fact that terms, containing time derivatives of the potential, are not systematically eliminated from deviations when such effective actions are used. If we use expressions derived for time-dependent potentials, as expected, the deviations are systematically reduced when we increase level p .

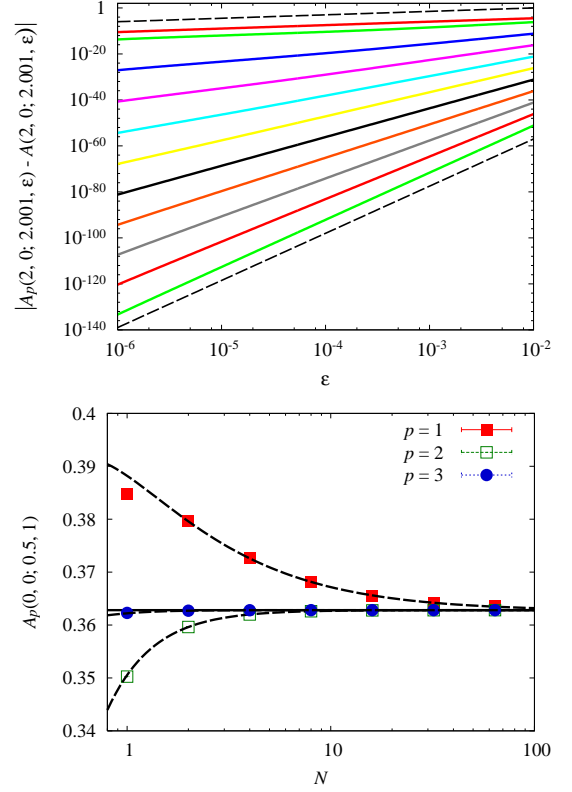


FIG. 3: (Color online) (top) Deviations $|A_p(2, 0; 2.001, \varepsilon) - A(2, 0; 2.001, \varepsilon)|$ as a function of propagation time ε for the forced harmonic oscillator (68) with $\omega = \Omega = 1$, calculated analytically for $p = 1, 2, 4, 6, 8, 10, 12, 14, 16, 18, 20$ from top to bottom. The dashed lines are proportional to $\varepsilon^{1.5}$ and $\varepsilon^{20.5}$, and demonstrate the perfect scaling of the corresponding level $p = 1$ and $p = 20$ results. (bottom) Convergence of numerical Monte-Carlo results for the transition amplitude $A_p(0, 0; 0.5, 1)$ as a function of the number of time steps N for $p = 1, 2, 3$. As before, dashed lines give the fitted functions $A_p + B_p/N^p + \dots$, demonstrating the expected $1/N^p$ scaling of the deviations. The number of Monte-Carlo samples was $N_{\text{MC}} = 2 \cdot 10^9$.

To show that the derived short-time effective actions can be used for calculating long-time transition amplitudes using the standard time discretization approach for path integrals, we display in Fig. 2 the convergence of the discretized long-time transition amplitude for the Grosche-rescaled harmonic oscillator as a function of the number of time steps N . As expected, we have obtained $1/N^p$ behavior, in accordance with our earlier conclusion on the N -scaling of errors in this case. The numerical results presented in this graph are obtained using the Monte Carlo SPEEDUP [52] code, which was modified to include time-dependent effective actions implemented to high orders in the C programming language.

The second exactly solvable model, which we have considered, is the forced harmonic oscillator [46],

$$V_{\text{FHO}}(x, t) = \frac{1}{2}\omega^2 x^2 - x \sin \Omega t, \quad (68)$$

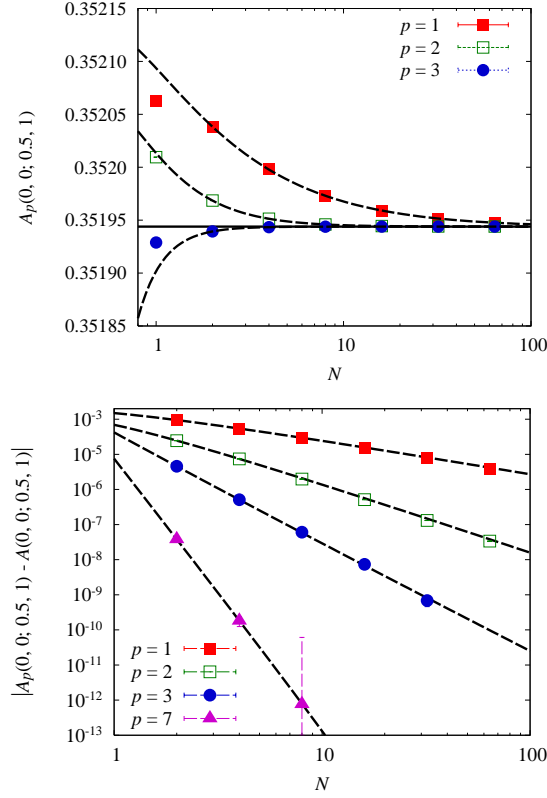


FIG. 4: (Color online) (top) Convergence of numerical Monte-Carlo results for the transition amplitude $A_p(0, 0; 0.5, 1)$ as a function of the number of time steps N for the pure quartic oscillator (69) with the anharmonicity $g = 0.1$, rescaled by the Grosche factor $\zeta(t) = \sqrt{1+t^2}$, and calculated with level $p = 1, 2, 3$ effective actions. As before, dashed lines give the fitted functions $A_p + B_p/N^p + \dots$ (bottom) In order to convincingly demonstrate the expected dominant $1/N^p$ behavior of deviations, we plot $|A_p(0, 0; 0.5, 1) - A(0, 0; 0.5, 1)|$ as a function of the number of time steps N for $p = 1, 2, 3, 7$. The dashed lines are fitted polynomials $A_p + B_p/N^p + \dots$, the same as on the top graph. The exact value of the amplitude is obtained as the constant term from fitting $p = 7$ results. The number of Monte-Carlo samples was $N_{MC} = 1.6 \cdot 10^{13}$ for $p = 7$, in order to be able to resolve the exceedingly small deviations from the exact value of the amplitude. For $p = 1, 2, 3$ we used much smaller values of N_{MC} , typically 10^8 to 10^{10} .

where Ω denotes the frequency of the external driving field. Fig. 3 presents numerical results for this model for $\omega = \Omega = 1$. The top plot gives deviations for the case of short-time transition amplitude, calculated analytically using level p effective action. We see again a perfect ε -scaling of deviations. The bottom plot shows convergence of a long-time transition amplitude as a function of the number of time steps N , illustrating the expected $1/N^p$ behavior.

We have numerically also considered the non-trivial case of a pure quartic oscillator $V_{PQ}(x) = gx^4/24$ rescaled

with the same Grosche factor $\zeta(t) = \sqrt{1+t^2}$:

$$V_{G,PQ}(x, t) = \frac{gx^4}{24(1+t^2)^3}. \quad (69)$$

This model is not exactly solvable, but the continuous transition amplitude can be determined numerically. To this end one could use the Grosche mapping, while relying on the previous numerical approach [34], providing exact transition amplitudes for the time-independent counterpart of the potential V_{PQ} . Another possibility is based on numerically obtained results from the modified SPEEDUP code, relying on the fitting of discretized amplitudes to the $\varepsilon \rightarrow 0$ limit. As we can see from Fig. 4, the numerical results exhibit a perfect scaling behavior for this non-trivial model as well. The power-law scaling of deviations in the calculated discretized transition amplitudes up to exceedingly small values fully verifies the presented analytic derivation of effective actions.

As we have demonstrated during our analysis of several examples, the main advantage of the effective action approach is the calculation of transition amplitudes with high precision, which can be improved by using higher levels p . While this favors the presented method in applications, where such high-precision transition amplitudes are necessary, e.g. the calculation of partition functions, other higher-order schemes may be preferred for solving different types of problems. For example, the split-operator method [21, 26–29, 43] is ideally suited for studying both the real- and the imaginary-time evolution of various quantum systems. Furthermore, it has the advantage that it can be implemented in any chosen representation, which is appropriate for the quantum system, while the effective action approach relies on using the coordinate representation.

D. Velocity Independent Part of the Effective Potential

Now we turn our attention to the special case of the velocity independent part of the effective potential, which we designate by $W_0(x; \varepsilon, \tau) \equiv W(x, 0; \varepsilon, \tau)$. It determines the diagonal amplitudes, for which the discretized velocity \bar{x} is equal to zero. The efficient and precise calculation of diagonal transition amplitudes is essential for many quantum statistical problems, since it provides a direct method to obtain partition functions, and can be used to calculate energy spectra, density profiles and other relevant physical quantities. Therefore, we will derive a new set of recursive relations for those coefficients $c_m \equiv c_{m,0}$ which determine the effective potential W_0 :

$$W_0(x; \varepsilon, \tau) = \sum_{m=0}^{\infty} c_m(x, \tau) \varepsilon^m. \quad (70)$$

Such recursive relations will turn out to be much simpler than the full set (49) and (50) obtained in the previous section.

In order to derive equations determining the coefficients c_m , we have to perform the limit $\bar{x} \rightarrow 0$ in the differential equation (46) for the effective potential W . This is nontrivial, since the equation contains derivatives with respect to \bar{x} . Therefore, we re-examine both Schrödinger equations (43) and (44) for the transition amplitude. If we take the derivative with respect to \bar{x} of the second equation, use it to express the term $\partial \bar{\partial}^2 A$, and insert it into the derivative of the first equation with respect to x , we obtain the differential equation

$$\begin{aligned} \partial_\varepsilon \partial A - \frac{1}{8} \partial^3 A - \frac{1}{4} \partial_\tau \bar{\partial} A - \frac{1}{4} A \bar{\partial} (V_+ - V_-) \\ + \frac{1}{2} A \partial (V_+ + V_-) - \frac{1}{4} (V_+ - V_-) \bar{\partial} A \\ + \frac{1}{2} (V_+ + V_-) \partial A = 0, \end{aligned} \quad (71)$$

in which it is easier to perform the required $\bar{x} \rightarrow 0$ limit. In the terms that do not contain derivatives with respect to \bar{x} , we can just set $\bar{x} = 0$ and replace the transition amplitude A with $A_0 = \exp(-\varepsilon W_0)/\sqrt{2\pi\varepsilon}$ due to (45). In the remaining terms the limit has to be performed more carefully. The terms containing combinations $V_+ \pm V_-$ and their derivatives are the simplest, and we obtain

$$(V_+ + V_-) \Big|_{\bar{x} \rightarrow 0} = 2 \sum_{m=0}^{\infty} \frac{\varepsilon^{2m} V^{(2m)}}{(2m)! 2^{2m}}, \quad (72)$$

$$(V_+ - V_-) \Big|_{\bar{x} \rightarrow 0} = 2 \sum_{m=0}^{\infty} \frac{\varepsilon^{2m+1} V^{(2m+1)}}{(2m+1)! 2^{2m+1}}, \quad (73)$$

$$\begin{aligned} \partial(V_+ + V_-) \Big|_{\bar{x} \rightarrow 0} &= \bar{\partial}(V_+ + V_-) \Big|_{\bar{x} \rightarrow 0} \\ &= 2 \sum_{m=0}^{\infty} \frac{\varepsilon^{2m} V^{(2m)'}}{(2m)! 2^{2m}}, \end{aligned} \quad (74)$$

where the prime in the last expression denotes the derivative with respect to x . For the terms $\bar{\partial} A$ and $\partial_\tau \bar{\partial} A$ we have to explicitly use the full double power expansion for the effective potential (32), perform the differentiation and take the limit afterwards. This yields the results

$$\bar{\partial} A \Big|_{\bar{x} \rightarrow 0} = -\varepsilon A_0 \sum_{m=0}^{\infty} c_{m+1/2} \varepsilon^m, \quad (75)$$

$$\partial_\tau \bar{\partial} A \Big|_{\bar{x} \rightarrow 0} = -\varepsilon A_0 \sum_{m=0}^{\infty} \varepsilon^m (\dot{c}_{m+1/2} - c_{m+1/2} \varepsilon \dot{W}_0), \quad (76)$$

where dots now represent derivatives with respect to the time argument τ of the coefficient $c_{m+1/2} \equiv c_{m+1/2,0}$ and the effective potential W_0 . As we see, the odd-power coefficients $c_{m+1/2}$ cannot be eliminated altogether, although we are considering the diagonal amplitudes, for which we have $\bar{x} = 0$. This is due to the derivatives with respect to \bar{x} . From this we can deduce that we will need again two recursion relations to determine all needed coefficients, despite the fact that in the end we will use only the even-power ones. Therefore, we will use Eq. (44) to derive the second recursive relation for the coefficients. In order to do so, we still need to calculate the term $\partial \bar{\partial} A$ in the considered limit $\bar{x} \rightarrow 0$:

$$\partial \bar{\partial} A \Big|_{\bar{x} \rightarrow 0} = A_0 \sum_{m=0}^{\infty} \varepsilon^m (c_{m+1/2} \varepsilon^2 W_0' - c_{m+1/2}' \varepsilon). \quad (77)$$

Inserting all calculated $\bar{x} \rightarrow 0$ terms into equations (71) and (44), as well as using the expansion (70), we finally obtain the following coupled system of recursive relations for the coefficients c_m and $c_{m+1/2}$:

$$\begin{aligned} (2m+1) c_m' &= \Pi(0, m) \frac{V^{(m)'}}{m! 2^m} + \frac{1}{4} c_{m-1}'' + \frac{1}{2} \dot{c}_{m-1/2} - 2 \sum_l \frac{V^{(2l)}}{(2l)! 2^{2l}} c_{m-2l-1}' + \sum_l \frac{V^{(2l+1)}}{(2l+1)! 2^{2l+1}} c_{m-2l-3/2} \\ &+ 2 \sum_l c_l' c_{m-l-1} + 2 \sum_l l c_l c_{m-l-1}' - \frac{3}{4} \sum_l c_l' c_{m-l-2}'' - \frac{1}{2} \sum_l c_{l+1/2} \dot{c}_{m-l-2} + \frac{1}{4} \sum_{l,r} c_l' c_r' c_{m-l-r-3}', \end{aligned} \quad (78)$$

$$\frac{1}{2} c_{m+1/2}' = -2 \Pi(0, m) \frac{V^{(m+1)'}}{(m+1)! 2^{m+1}} + \dot{c}_m + \frac{1}{2} \sum_l c_{l+1/2} c_{m-l-1}'. \quad (79)$$

The above recursive relations are solved in a similar way as before. In order to obtain the level p diagonal effective action W_0 , we need to take into account the terms in the expansion with $m = 0, 1, \dots, p-1$. The recursions for c_m' and $c_{m+1/2}'$ are easily solved starting from $m = 0$ to a desired level $p-1$. Although we get in this way only

their first derivatives with respect to x , the coefficients themselves can be calculated by direct symbolic integration, and all solutions can be expressed in a closed form. The explicit calculation of the coefficients to high orders yields the same results we have obtained in the previous

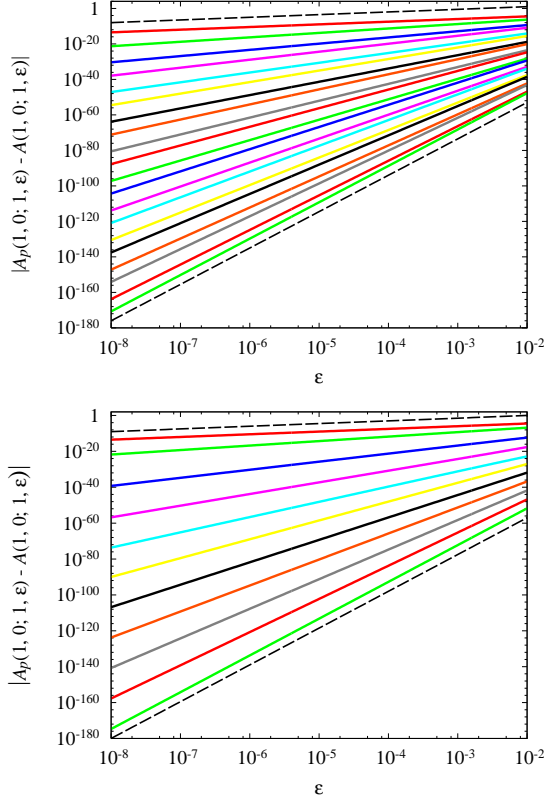


FIG. 5: (Color online) Deviations of diagonal transition amplitudes $|A_p(1, 0; 1, \varepsilon) - A(1, 0; 1, \varepsilon)|$ as a function of propagation time ε for: (top) time-dependent harmonic oscillator (67), calculated analytically for $p = 1, 2, 3, 4, \dots, 20$ from top to bottom; (bottom) forced harmonic oscillator (68) with $\omega = 1$ and $\Omega = 2$, calculated analytically for $p = 1, 2, 4, 6, 8, 10, 12, 14, 16, 18, 20$ from top to bottom. The dashed lines on both graphs are proportional to $\varepsilon^{1.5}$ and $\varepsilon^{20.5}$, and demonstrate the perfect scaling of the corresponding level $p = 1$ and $p = 20$ results.

section. To order $p = 1$, we only have the trivial equation

$$c'_0 = V', \quad (80)$$

that gives the well-known boundary condition $c_0 = V$. To order $p = 2$ we have

$$c'_{1/2} = -2\dot{V} + 2\dot{c}_0 = 0, \quad (81)$$

$$3c'_1 = \frac{1}{4}c'''_0 + \frac{1}{2}\dot{c}_{1/2} - 2Vc'_0 + 2c'_0c_0 = \frac{1}{4}c'''_0, \quad (82)$$

which corresponds to the result in Eq. (55). To order $p = 3$ we first calculate the odd-power coefficient,

$$c'_{3/2} = 2\dot{c}_1 + c_{1/2}c'_0 = \frac{1}{6}c''_0, \quad (83)$$

which leads to the result (56). The even-power coefficient

c_2 is obtained from

$$\begin{aligned} 5c'_2 &= \frac{1}{8}\ddot{V}' + \frac{1}{4}c'''_1 + \frac{1}{2}\dot{c}_{3/2} - 2Vc'_1 + \frac{1}{2}\dot{V}c_{1/2} + 4c'_0c_1 \\ &\quad + 2c'_1c_0 - \frac{1}{2}c_{1/2}\dot{c}_0 - \frac{3}{4}c'_0c''_0 \\ &= \left(\frac{1}{48}V^{(4)} - \frac{5}{24}V'^2 + \frac{5}{24}\ddot{V} \right)', \end{aligned} \quad (84)$$

which coincides with the result in Eq. (59). We similarly proceed to calculate higher-order coefficients. This is easily automated in symbolic calculus software packages like Mathematica [51].

The main advantage of this approach is that we have been able to derive recursion relations involving only the lower-level coefficients $c_m = c_{m,0}$ and $c_{m+1/2} = c_{m+1/2,0}$, thus not requiring the calculation of all even- and odd-power coefficients, which are needed for the general case. At the end of this section, we note that for time-independent potential V the recursive relation (78) reduces to the previously known result [34], while the second recursion (79) yields the expected result $c_{m+1/2} = 0$. Note that our recursive approach thus allows to calculate higher orders of the so-called Wigner expansion [56].

Fig. 5 illustrates practical advantages of using velocity-independent effective actions for the numerical calculation of diagonal transition amplitudes. The top plot gives the deviations of diagonal amplitudes calculated with different levels p of the effective potential W_0 for the Grosche-rescaled harmonic oscillator (67), while the bottom plot gives the analogous results for the forced harmonic oscillator (68). The obtained ε -scaling to exceedingly high orders p demonstrates the correctness of the analytically derived results.

V. MULTI-COMPONENT SYSTEMS

Now we extend the calculations of Sec. IV B to the case of a general multi-component non-relativistic quantum system of P particles in d dimensions. Note that such a formalism is needed even for studies of single-particle systems in two or three spatial dimensions, which have more than one degree of freedom. For example, time-independent many-body effective actions of level $p = 21$ have already been used for a numerical study of fast-rotating Bose-Einstein condensates [38], as well as a high-precision calculation of the energy spectra and eigenfunctions of several two-dimensional models [37]. The presented extension of the many-body formalism will allow studies of such systems in external time-dependent potentials, as well as the investigation of the formation and evolution of vortices [6, 7] and other dynamical phenomena. We also plan to study collective oscillation modes of Bose-Einstein condensates with a parametrically modulated interaction [58].

To develop the time-dependent many-body formalism, we solve the differential equation (46) for the effective

potential W by using a multi-dimensional many-particle generalization of the double power expansion (32)

$$W(\mathbf{x}, \bar{\mathbf{x}}; \varepsilon, \tau) = \sum_{m=0}^{\infty} \sum_{k=0}^m \left\{ W_{m,k}(\mathbf{x}, \bar{\mathbf{x}}; \tau) \varepsilon^{m-k} + W_{m+1/2,k}(\mathbf{x}, \bar{\mathbf{x}}; \tau) \varepsilon^{m-k} \right\}. \quad (85)$$

Here we have introduced the contractions

$$W_{m,k}(\mathbf{x}, \bar{\mathbf{x}}; \tau) = \bar{x}_{i_1} \cdots \bar{x}_{i_{2k}} c_{m,k}^{i_1, \dots, i_{2k}}(\mathbf{x}; \tau), \quad (86)$$

$$W_{m+1/2,k}(\mathbf{x}, \bar{\mathbf{x}}; \tau) = \bar{x}_{i_1} \cdots \bar{x}_{i_{2k+1}} c_{m+1/2,k}^{i_1, \dots, i_{2k+1}}(\mathbf{x}; \tau), \quad (87)$$

in such a way that they correspond to the case of the time-independent potential [34]. In the above relations we assume the Einstein convention that summation over repeated indices is performed. The introduction of such contractions of tensorial coefficients c significantly simplifies in this case the analytic derivation and also provides a key ingredient for implementing the many-body recursion relations in symbolic calculations using Mathematica. Otherwise, the task to explicitly symmetrize the

coefficients would amount to a complexity of the algorithm which scales with the number of possible permutations $(Pd)!$ and which would not be feasible even for a very moderate number of particles. Using scalar quantities, which are obtained by contracting the coefficients with the discretized velocity $\bar{\mathbf{x}} = \boldsymbol{\delta}/2$, efficiently solves this problem.

The multi-dimensional analogue of expression (48) has the form

$$\begin{aligned} & \frac{1}{2} (V_+ + V_-) \\ &= \sum_{m=0}^{\infty} \sum_{k=0}^m \left\{ \frac{\Pi(m,k) \varepsilon^{m-k}}{(2k)! (m-k)! 2^{m-k}} (\bar{\mathbf{x}} \cdot \boldsymbol{\partial})^{2k} \frac{(m-k)}{V} \right. \\ & \quad \left. + \frac{(1 - \Pi(m,k)) \varepsilon^{m-k}}{(2k+1)! (m-k)! 2^{m-k}} (\bar{\mathbf{x}} \cdot \boldsymbol{\partial})^{2k+1} \frac{(m-k)}{V} \right\}, \quad (88) \end{aligned}$$

and after inserting it into the differential equation for the effective potential we obtain recursive relations for even- and odd-power contractions $W_{m,k}$ and $W_{m+1/2,k}$:

$$8(m+k+1) W_{m,k} = 8 \frac{\Pi(m,k) (\bar{\mathbf{x}} \cdot \boldsymbol{\partial})^{2k} V^{(m-k)}}{(2k)! (m-k)! 2^{m-k}} + \bar{\partial}^2 W_{m,k+1} + \partial^2 W_{m-1,k} - \sum_{l,r} \left\{ \partial W_{l,r} \cdot \partial W_{m-l-2,k-r} + \right. \quad (89)$$

$$\left. \partial W_{l+1/2,r} \cdot \partial W_{m-l-5/2,k-r-1} + \bar{\partial} W_{l,r} \cdot \bar{\partial} W_{m-l-1,k-r+1} + \bar{\partial} W_{l+1/2,r} \cdot \bar{\partial} W_{m-l-3/2,k-r} \right\},$$

$$\begin{aligned} 8(m+k+2) W_{m+1/2,k} &= 8 \frac{(1 - \Pi(m,k)) (\bar{\mathbf{x}} \cdot \boldsymbol{\partial})^{2k+1} V^{(m-k)}}{(2k+1)! (m-k)! 2^{m-k}} + \bar{\partial}^2 W_{m+1/2,k+1} + \partial^2 W_{m-1/2,k} - \\ & \sum_{l,r} \left\{ \partial W_{l,r} \cdot \partial W_{m-l-3/2,k-r} + \partial W_{l+1/2,r} \cdot \partial W_{m-l-2,k-r} + \bar{\partial} W_{l+1/2,r} \cdot \bar{\partial} W_{m-l-1,k-r+1} + \bar{\partial} W_{l,r} \cdot \bar{\partial} W_{m-l-1/2,k-r+1} \right\}. \quad (90) \end{aligned}$$

The diagonal contractions can easily be calculated in a closed form as in the single-particle one-dimensional case,

$$W_{m,m} = \frac{1}{(2m+1)!} (\bar{\mathbf{x}} \cdot \boldsymbol{\partial})^{2m} V, \quad (91)$$

$$W_{m+1/2,m} = 0. \quad (92)$$

Thus, the recursion relations (89) and (90) can be solved up to a given order p together with (91) and (92) by using a similar procedure. Here we give the solution up to order $p = 4$, which generalizes the previously given solution for the simple case $P = d = 1$. For $m = 0$ we only have the naive $p = 1$ term, i.e.

$$W_{0,0} = V, \quad (93)$$

while $m = 1$ yields the first non-trivial even-power terms

$$W_{1,1} = \frac{1}{6} (\bar{\mathbf{x}} \cdot \boldsymbol{\partial})^2 V, \quad (94)$$

$$W_{1,0} = \frac{1}{12} \partial^2 V, \quad (95)$$

which are sufficient to construct $p = 2$ effective action. The next term we calculate is the odd-power contraction for $m = 1$, i.e.

$$W_{3/2,0} = \frac{1}{6} (\bar{\mathbf{x}} \cdot \boldsymbol{\partial}) \dot{V}, \quad (96)$$

which contains the explicit time derivative of V . For

$m = 2$ we obtain the next order of even-power terms:

$$W_{2,2} = \frac{1}{120} (\bar{\mathbf{x}} \cdot \boldsymbol{\partial})^4 V, \quad (97)$$

$$W_{2,1} = \frac{1}{120} (\bar{\mathbf{x}} \cdot \boldsymbol{\partial})^2 \partial^2 V, \quad (98)$$

$$W_{2,0} = \frac{1}{24} \ddot{V} + \frac{1}{240} \partial^4 V - \frac{1}{24} (\partial V)^2. \quad (99)$$

These terms, together with the previously calculated ones, are sufficient to construct level $p = 3$ effective action. In order to be able to complete $p = 4$ effective action derivation, we still need to calculate odd-power contractions corresponding to $m = 2$

$$W_{5/2,1} = \frac{1}{60} (\bar{\mathbf{x}} \cdot \boldsymbol{\partial})^3 \dot{V}, \quad (100)$$

$$W_{5/2,0} = \frac{1}{120} (\bar{\mathbf{x}} \cdot \boldsymbol{\partial}) \partial^2 \dot{V}, \quad (101)$$

$$(102)$$

as well as even-power contractions for $m = 3$,

$$W_{3,3} = \frac{1}{5040} (\bar{\mathbf{x}} \cdot \boldsymbol{\partial})^6 V, \quad (103)$$

$$W_{3,2} = \frac{1}{3360} (\bar{\mathbf{x}} \cdot \boldsymbol{\partial})^4 \partial^2 V, \quad (104)$$

$$W_{3,1} = \frac{1}{3360} (\bar{\mathbf{x}} \cdot \boldsymbol{\partial})^2 \partial^4 V + \frac{1}{80} (\bar{\mathbf{x}} \cdot \boldsymbol{\partial})^2 \ddot{V} \quad (105)$$

$$\begin{aligned} & - \frac{1}{360} [(\bar{\mathbf{x}} \cdot \boldsymbol{\partial}) \partial V]^2 - \frac{1}{120} (\partial V) \cdot (\bar{\mathbf{x}} \cdot \boldsymbol{\partial})^2 \partial V, \\ W_{3,0} = & \frac{1}{6720} \partial^6 V + \frac{1}{480} \partial^2 \ddot{V} - \frac{1}{360} (\partial_i \partial V) \cdot (\partial_i \partial V) \\ & - \frac{1}{120} (\partial V) \cdot \partial^2 \partial V. \end{aligned} \quad (106)$$

This concludes the calculation of level $p = 4$ effective action for a general many-body quantum system. As before, the obtained results automatically reduce to already known effective actions for the time-independent potentials [34] if we set all time-derivatives of the potential to zero. Furthermore, the many-body results (93)–(106) reduce for the special case $P = d = 1$ to the previous results (53)–(65).

In order to numerically verify the developed expressions for the case of multi-component quantum systems, we will calculate transition amplitudes of a set of time-dependent harmonic oscillators,

$$V(\mathbf{q}, t) = \sum_{i=1}^P \frac{1}{2} \omega_i^2(t) q_i^2, \quad (107)$$

which represents the archetypical model for many physical phenomena. This exactly solvable model allows us to compare analytical expressions obtained from recursive relations and to verify that using level p effective action leads to values of transition amplitudes which are correct up to order $\varepsilon^{p+1-Pd/2}$. As we can see in Fig. 6 for a system of $P = 2, 4, 6$ time-dependent oscillators, the respective scaling is perfect. The middle and bottom plots

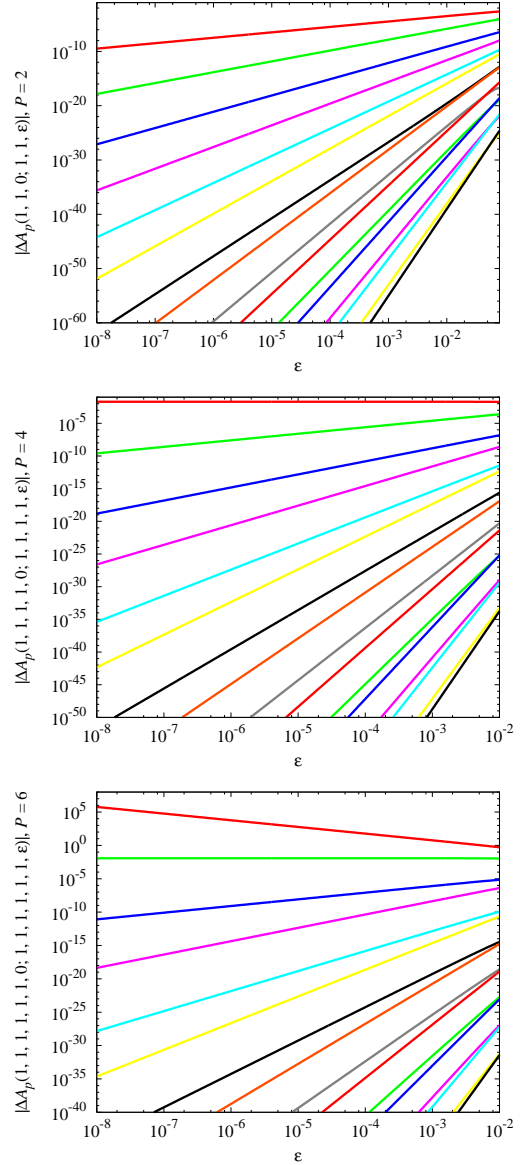


FIG. 6: (Color online) Deviations of diagonal transition amplitudes $|\Delta A_p(\mathbf{a} = \mathbf{1}, t_a = 0; \mathbf{b} = \mathbf{1}, t_b = \varepsilon)|$ from the exact values as a function of propagation time ε for a multi-component system (107) of time-dependent harmonic oscillators: (top) $P = 2$ oscillators, with $\omega_1^2(t) = 1 + \frac{1}{2} \sin^2 2t$, $\omega_2^2(t) = 1 + \frac{1}{2} \cos 2t$; (middle) $P = 4$ oscillators, with $\omega_1^2(t)$, $\omega_2^2(t)$, $\omega_3^2(t) = 2 + \cos 5t$, $\omega_4^2(t) = 4 + \sin^2 4t$; (bottom) $P = 6$ oscillators, with $\omega_1^2(t)$, $\omega_2^2(t)$, $\omega_3^2(t)$, $\omega_4^2(t)$, $\omega_5^2(t) = 2 + \sin^2 t$, $\omega_6^2(t) = 4 + 2 \cos 3t$. Each plot gives results for transition amplitudes calculated using the effective action levels $p = 1, 2, \dots, 16$, from top to bottom.

illustrate another important feature of the short-time expansion for multi-component systems: as the number of components of the system Pd increases, the exponent $p + 1 - Pd/2$ may become zero or negative for a given effective action level p . This leads to the peculiar behavior observed in the middle and bottom plots for small values

of p , with the deviation of the amplitude being constant ($P = 4$, $p = 1$ in the middle plot, $P = 6$, $p = 2$ in the bottom plot) or even increasing ($P = 6$, $p = 1$ in the bottom plot) when ε is decreased. Thus this prevents the calculation of the transition amplitude with high accuracy, which is, in principle, expected to be possible by decreasing ε . As we see, to enable such high-accuracy calculations, one has to use an effective action with sufficiently high level p . The important contribution of the presented approach lies in the fact that it offers a systematic formalism for deriving such higher order expressions for a general quantum multi-component system.

Finally, we emphasize that the obtained discretized effective actions can be used for solving a plethora of non-equilibrium many-body quantum problems within the exact diagonalization [36, 37] or Path-Integral Monte-Carlo approach, including the continuous-space worm algorithm [57]. For instance, in typical experimental setups with ultracold quantum gases harmonic or anharmonic confining potentials are generically switched on and off, thus generating natural non-equilibrium situations. As so far mainly quenched potentials have been considered, it would certainly be rewarding to study in a systematic way how the time scale, upon which a potential is switched off, influences the observed time-of-flight absorption pictures. Another upcoming research field is the investigation of the phenomenon of parametric resonance in Bose-Einstein condensates. A first experiment, where the s-wave scattering length of ^7Li atoms has been modulated periodically with the help of a Feshbach resonance, has recently been performed [58]. In order to understand the observed resonance spectrum both analytical methods from nonlinear dynamics [59] and numerical methods as the presented fast converging path-integral approach have to be combined.

VI. REAL-TIME FORMALISM

The presented approach has so far been developed within the imaginary-time framework, which is useful in many practical applications. However, in order to study the more relevant real-time dynamics of quantum systems, we have to switch back to the real-time formalism. One possibility would be to make all calculations in imaginary time, and then to try to perform an inverse Wick rotation, which might be difficult due to various reasons mentioned in Sec. II. Another, much more straight-forward possibility is to derive a new set of recursive relations within the real-time formalism. In this section we will briefly outline such a procedure.

Reverting the imaginary-time formalism into a real-time one is easily achieved by replacing the variable t representing the imaginary time with it_{R} in all expressions, where now t_{R} represents the real time. This includes also the replacement of the time-interval ε with $i\varepsilon_{\text{R}}$, and the time-midpoint τ with its real-time counterpart $i\tau_{\text{R}}$. The

short-time transition amplitude is now expressed as

$$A(\mathbf{a}, t_a; \mathbf{b}, t_b) = \frac{1}{(2\pi i\varepsilon_{\text{R}})^{Pd/2}} e^{iS^*(\mathbf{x}, \boldsymbol{\delta}; \varepsilon_{\text{R}}, \tau_{\text{R}})}, \quad (108)$$

and the effective action as

$$S^*(\mathbf{x}, \boldsymbol{\delta}; \varepsilon_{\text{R}}, \tau_{\text{R}}) = \frac{\delta^2}{2\varepsilon_{\text{R}}} - \varepsilon_{\text{R}} W(\mathbf{x}, \boldsymbol{\delta}; \varepsilon_{\text{R}}, \tau_{\text{R}}), \quad (109)$$

representing real-time versions of Eqs. (13) and (14), respectively. Following the same procedure as in Sec. III, we arrive at the real-time counterpart of Eq. (46) for the effective potential,

$$W + \bar{\mathbf{x}} \cdot \bar{\partial} W + \varepsilon \partial_{\varepsilon} W - \frac{i}{8} \varepsilon \partial^2 W - \frac{i}{8} \varepsilon \bar{\partial}^2 W - \frac{1}{8} \varepsilon^2 (\partial W)^2 - \frac{1}{8} \varepsilon^2 (\bar{\partial} W)^2 = \frac{1}{2} (V_+ + V_-). \quad (110)$$

where the subscript R is dropped for simplicity. Further derivation of real-time recursion relations is a straight-forward task. For brevity, we will not give the explicit form of the recursion relations, but their Mathematica implementation is available from the SPEEDUP code web page [52].

We will illustrate the applicability of this formalism for studying the real-time dynamics within the space-discretized approach [36, 37]. If we discretize the continuous space and replace it with a grid defined by a discretization step Δ , all quantities are only defined on a discrete set of coordinates $\mathbf{q}_{\mathbf{n}} = \mathbf{n}\Delta$, where $\mathbf{n} \in \mathbb{Z}^{Pd}$ is a vector of Pd integer numbers. Matrix elements of the evolution operator,

$$U_{\mathbf{nm}}(t_a \rightarrow t_b) = \langle \mathbf{q}_{\mathbf{n}} | \hat{U}(t_a \rightarrow t_b) | \mathbf{q}_{\mathbf{m}} \rangle, \quad (111)$$

represent real-time transition amplitudes $A_{\mathbf{nm}}(t_a, t_b) = A(\mathbf{q}_{\mathbf{n}}, t_a; \mathbf{q}_{\mathbf{m}}, t_b)$, which can be calculated using the real-time effective action approach. If the initial state of the system $|\psi, t_a\rangle$ is represented by a vector $\psi(t_a)$ whose elements are $\psi_{\mathbf{n}}(t_a) = \psi(\mathbf{q}_{\mathbf{n}}, t_a) = \langle \mathbf{q}_{\mathbf{n}} | \psi, t_a \rangle$, its dynamics can be calculated by a simple matrix multiplication $\psi(t_b) = U(t_a \rightarrow t_b) \cdot \psi(t_a)$, i.e.

$$\psi_{\mathbf{n}}(t_b) = \sum_{\mathbf{m}} U_{\mathbf{nm}}(t_a \rightarrow t_b) \psi_{\mathbf{m}}(t_a). \quad (112)$$

Therefore, since the matrix elements of the evolution operator can be accurately calculated using the effective action approach, we are able to study real-time dynamics of the system starting from any desired initial state.

Note that, although we rely on the short-time expansion of transition amplitudes, we are not limited to study only a short-time evolution, since the above matrix multiplication can be repeatedly performed. For any given propagation time T , we can divide the evolution to N sub-intervals of length $\varepsilon = T/N$, which now correspond to short-time evolution matrix elements $U_{\mathbf{nm}}(\varepsilon)$. In addition to this, using the higher-order effective actions makes

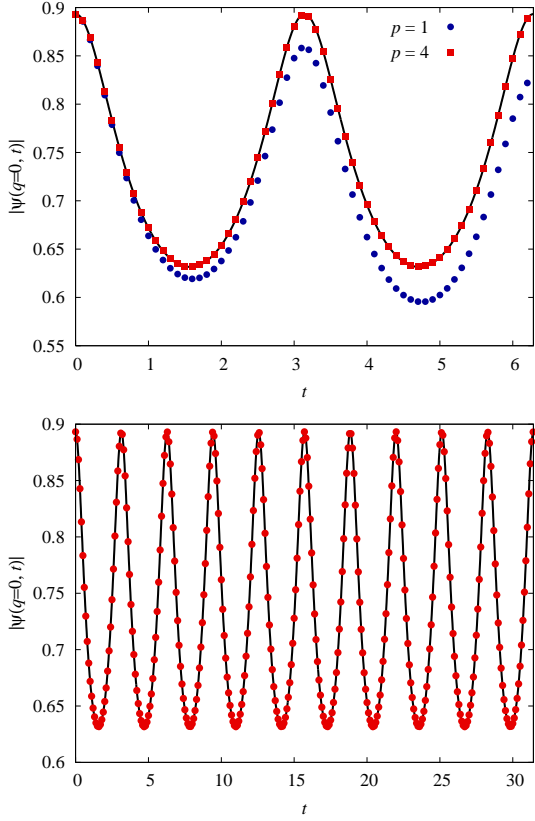


FIG. 7: (Color online) Time evolution of the one-dimensional harmonic oscillator $V(q) = \frac{1}{2}\omega^2 q^2$ calculated using the space-discretized method [36, 37] and the effective action approach with: (top) $p = 1, 4$ and (bottom) $p = 20$. Both graphs display the time dependence $|\psi(q=0, t)|$ of the absolute value of the wave function at $q = 0$, and solid line represents the exact solution. The harmonic frequency was $\omega = 1$, the time-interval for propagation was $\varepsilon = 0.1$, and the initial state was set to the ground state of the harmonic oscillator with $\omega = 2$.

it possible to perform high-accuracy calculations of U_{nm} , and, correspondingly, to eliminate the associated numerical errors for all practical purposes.

To demonstrate this, we show in Fig. 7 the time evolution of a harmonic oscillator $V(q) = \frac{1}{2}\omega^2 q^2$ calculated using the described method with effective action levels $p = 1, 4$ and $p = 20$. As we can see, using the propagation interval $\varepsilon = 0.1$, the naive $p = 1$ action can be used only for short propagations times, while we are able to reproduce very accurately the long-time evolution of the system with higher p levels. In order to further quantitatively assess numerical errors of the obtained results, we use the following integral measure,

$$\|\psi(t) - \psi_p(t)\| = \left(\int_{-\infty}^{\infty} |\psi(q, t) - \psi_p(q, t)|^2 dq \right)^{1/2}, \quad (113)$$

where $\psi(q, t)$ represents the exact time evolution of the wave function, and $\psi_p(q, t)$ is the approximate time evolution calculated using level p effective action. The semi-

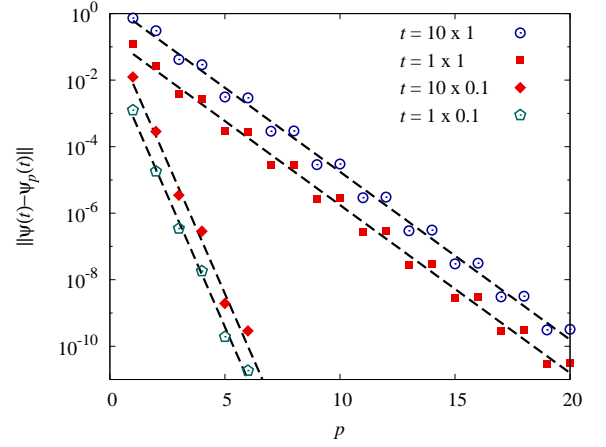


FIG. 8: (Color online) Integral measure (113) for numerically calculated time evolution of the harmonic oscillator as a function of the effective action level p for different values of the propagation time t . The parameters are the same as in Fig. 7.

log plot in Fig. 8 gives the p -dependence of the above-defined integral measure and demonstrates that it obeys the expected power law, i.e. $\varepsilon^{p+1/2}$ in this case, leading to a much smaller error when the propagation interval is reduced from $\varepsilon = 1$ to $\varepsilon = 0.1$. This graph also shows that errors due to the repeated matrix multiplication accumulate linearly with the number of time steps.

The study of errors presented in Fig. 8 is very instrumental in the optimization of numerical parameters in practical applications. If we compare errors which correspond to the same total evolution time $t = 1$, calculated for a propagation in one time-step $\varepsilon = t$ and in $N = 10$ steps $\varepsilon = t/N$, we can see that decreasing ε substantially reduces errors. This is easily understood, since errors are proportional to $\varepsilon^{p+1-Pd/2}$ and, therefore, introducing N time steps is expected to reduce errors by a factor of $N^{p+1-Pd/2}$. However, the fact that the matrix multiplication will have to be repeated N times introduces an additional factor of N , thus leading to the total reduction factor of $N^{p-Pd/2}$.

As a final example, we calculate the time evolution of the time-dependent harmonic oscillator with the potential

$$V(q, t) = \frac{1}{2}\omega^2(t)q^2 \quad (114)$$

with the frequency $\omega(t) = 1 + \frac{1}{10}t$ for $p = 1$ and $p = 6$. Fig. 9 displays time evolution of the absolute value of the wave function at $q = 0$ with the propagation interval $\varepsilon = 0.1$, and the initial state set to

$$\psi(q, t=0) = \frac{1}{\pi^{1/4}} e^{-\frac{1}{2}q^2 + \frac{1}{2}iq}. \quad (115)$$

As expected, the naive $p = 1$ effective action can be only used for very short propagation times, while $p = 2$ action gives accurate results for longer propagation times $T \leq 15$. A moderate level $p = 6$ effective action represents a

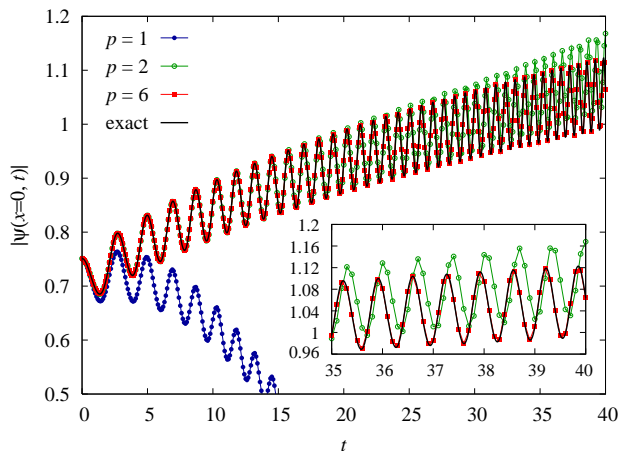


FIG. 9: (Color online) Time evolution of the time-dependent harmonic oscillator (114) calculated using the space-discretized method [36, 37] and the effective action approach with $p = 1$, $p = 2$ and $p = 6$. The graph displays the time dependence $|\psi(q = 0, t)|$ of the absolute value of the wave function at $q = 0$. The time-dependent harmonic frequency is given by $\omega(t) = 1 + \frac{1}{10}t$, time-interval for propagation was $\varepsilon = 0.1$, and the initial state was set according to Eq. (115).

substantial improvement and can be used to accurately study much longer propagation times.

VII. CONCLUSIONS

We have presented an analytic procedure for deriving the short-time expansion of the propagator for a gen-

eral non-relativistic quantum system with many degrees of freedom in a time-dependent potential up to previously inaccessible high orders. The procedure is based on recursively solving both the forward and backward Schrödinger equation for the transition amplitude. Following an earlier approach for time-independent potentials [34], we have derived recursion relations which allow an efficient analytic calculation of the effective potential to arbitrarily high order in the propagation time ε in the imaginary as well as in the real-time formalism. The analytically derived results are verified by studying several simple models. Finally, a list of possible applications of the presented method to relevant many-body quantum systems has been briefly outlined.

Acknowledgements

We thank Hagen Kleinert for several useful suggestions. This work was supported in part by the Ministry of Science and Technological Development of the Republic of Serbia, under project No. ON141035, ON171017 and bilateral project PI-BEC funded jointly with the German Academic Exchange Service (DAAD), and the European Commission under EU Centre of Excellence grant CX-CMCS. Numerical simulations were run on the AEGIS e-Infrastructure, supported in part by FP7 project EGI-InSPIRE, HP-SEE and PRACE-IIP.

-
- [1] V. Bretin, S. Stock, Y. Seurin, and J. Dalibard, Phys. Rev. Lett. **92**, 050403 (2004).
 - [2] A. L. Fetter, B. Jackson, and S. Stringari, Phys. Rev. A **71**, 013605 (2005).
 - [3] S. Kling and A. Pelster, Phys. Rev. A **76**, 023609 (2007).
 - [4] S. Kling and A. Pelster, Laser Phys. **19**, 1072 (2009).
 - [5] P. Mason and N. G. Berloff, Phys. Rev. A **79**, 043620 (2009).
 - [6] A. Aftalion, X. Blanc, and J. Dalibard, Phys. Rev. A **71**, 023611 (2005).
 - [7] A. Aftalion, X. Blanc, and N. Lerner, Phys. Rev. A **79**, 011603(R) (2009).
 - [8] L. Fallani, L. De Sarlo, J. E. Lye, M. Modugno, R. Saers, C. Fort, and M. Inguscio, Phys. Rev. Lett. **93**, 140406 (2004).
 - [9] D. E. Miller, J. K. Chin, C. A. Stan, Y. Liu, W. Setiawan, C. Sanner, and W. Ketterle, Phys. Rev. Lett. **99**, 070402 (2007).
 - [10] J. Mun, P. Medley, G. K. Campbell, L. G. Marcassa, D. E. Pritchard, and W. Ketterle Phys. Rev. Lett. **99**, 150604 (2007).
 - [11] E. Deumens, A. Diz, R. Longo, and Y. Öhrn, Rev. Mod. Phys. **66**, 917 (1994).
 - [12] T. Boness, S. Bose, and T. S. Monteiro, Phys. Rev. Lett. **96**, 187201 (2006).
 - [13] V. Eisler and I. Peschel, Annalen der Physik **17**, 410 (2008).
 - [14] B. Bellomo, R. LoFranco, S. Maniscalco, and G. Compagno, Phys. Rev. A **78**, 060302(R) (2008).
 - [15] P. Muruganandam and S. K. Adhikari, Comm. Phys. Comm. **180**, 1888 (2009).
 - [16] U. Schollwöck, Rev. Mod. Phys. **77**, 259 (2005).
 - [17] K. Hallberg, Adv. Phys. **55**, 477 (2006).
 - [18] E. Runge and E. K. U. Gross, Phys. Rev. Lett. **52**, 997 (1984).
 - [19] G. Onida, L. Reining, and A. Rubio, Rev. Mod. Phys. **74**, 601 (2002).
 - [20] K. Pernal, O. Gritsenko, and E. J. Baerends, Phys. Rev. A **75**, 012506 (2007).
 - [21] S. A. Chin and E. Krotscheck, Phys. Rev. E **72**, 036705 (2005).
 - [22] E. R. Hernández, S. Janecek, M. Kaczmarek, and E. Krotscheck, Phys. Rev. B **75**, 075108 (2007).
 - [23] O. Ciftja and S. A. Chin, Phys. Rev. B **68**, 134510 (2003).
 - [24] K. Sakkos, J. Casulleras, and J. Boronat, J. Chem. Phys. **130**, 204109 (2009).

- [25] A. D. Bandrauk and H. Shen, J. Chem. Phys. **99**, 1185 (1993).
- [26] S. A. Chin and C. R. Chen, J. Chem. Phys. **117**, 1409 (2002).
- [27] I. P. Omelyan, I. M. Mryglod, and R. Folk, Phys. Rev. E **66**, 026701 (2002).
- [28] I. P. Omelyan, I. M. Mryglod, and R. Folk, Comput. Phys. Commun. **151**, 272 (2003).
- [29] G. Goldstein and D. Baye, Phys. Rev. E **70**, 056703 (2004).
- [30] R. E. Zillich, J. M. Mayrhofer, and S. A. Chin, J. Chem. Phys. **132**, 044103 (2010).
- [31] A. Bogojević, A. Balaž, and A. Belić, Phys. Rev. Lett. **94**, 180403 (2005).
- [32] A. Bogojević, A. Balaž, and A. Belić, Phys. Rev. B **72**, 064302 (2005).
- [33] A. Bogojević, I. Vidanović, A. Balaž, and A. Belić, Phys. Lett. A **372**, 3341 (2008).
- [34] A. Balaž, A. Bogojević, I. Vidanović, and A. Pelster, Phys. Rev. E **79**, 036701 (2009).
- [35] D. Stojiljković, A. Bogojević, and A. Balaž, Phys. Lett. A **360**, 205 (2006).
- [36] I. Vidanović, A. Bogojević, and A. Belić, Phys. Rev. E **80**, 066705 (2009).
- [37] I. Vidanović, A. Bogojević, A. Balaž, and A. Belić, Phys. Rev. E **80**, 066706 (2009).
- [38] A. Balaž, I. Vidanović, A. Bogojević, and A. Pelster, Phys. Lett. A **374**, 1539 (2010).
- [39] K. Symanzik, in "Mathematical problems in theoretical physics", ed R. Schrader et al., Conf. Berlin 1981 (Springer, Berlin, 1982) Lecture notes in physics, Vol. **153**.
- [40] D. Fliegner, M. G. Schmidt, and C. Schubert, Z. Phys. C **64**, 111 (1994).
- [41] Q. Sheng, IMA J. Numer. Anal. **9**, 199 (1989).
- [42] M. Suzuki, J. Math. Phys. **32**, 400 (1991).
- [43] S. A. Chin, S. Janecek, and E. Krotscheck, Comp. Phys. Comm. **180**, 1700 (2009).
- [44] A. Bogojević, A. Balaž, and A. Belić, Phys. Rev. E **72**, 036128 (2005).
- [45] R. P. Feynman, Rev. Mod. Phys. **20**, 367 (1948).
- [46] R. P. Feynman and A. R. Hibbs, *Quantum Mechanics and Path Integrals* (McGraw-Hill, New York, 1965).
- [47] R. P. Feynman, *Statistical Mechanics* (Benjamin, New York, 1972).
- [48] H. Kleinert, *Path Integrals in Quantum Mechanics, Statistics, Polymer Physics, and Financial Markets*, 5th ed. (World Scientific, Singapore, 2009).
- [49] D. M. Ceperley, Rev. Mod. Phys. **67**, 279 (1995).
- [50] A. Bogojević, A. Balaž, and A. Belić, Phys. Lett. A **344**, 84 (2005).
- [51] Mathematica software package, <http://www.wolfram.com/mathematica/>
- [52] SPEEDUP C language and Mathematica code, <http://www.scl.rs/speedup/>
- [53] C. Grosche, Phys. Lett. A **182**, 28 (1993).
- [54] S. N. Storchak, Phys. Lett. A **135**, 77 (1989).
- [55] A. Pelster and A. Wunderlin, Z. Phys. B **89**, 373 (1992).
- [56] M. Hillary, R. F. O'Connell, M. O. Scully, and E. P. Wigner, Phys. Rep. **106**, 122 (1984).
- [57] M. Boninsegni, Nikolay Prokofev-, and B. Svistunov, Phys. Rev. Lett. **96**, 070601 (2006).
- [58] S. E. Pollack, D. Dries, R. G. Hulet, K. M. F. Magalhães, E. A. L. Henn, E. R. F. Ramos, M. A. Caracanhas, and V. S. Bagnato, Phys. Rev. A **81**, 053627 (2010).
- [59] F. K. Abdullaev, R. M. Galimzyanov, M. Brtko, and R. A. Kraenkel, J. Phys. B **37**, 3535 (2004).